2005-01-29

Influence of Electromyogram (EMG) Amplitude Processing in EMG-Torque Estimation

Oljeta Bida
Worcester Polytechnic Institute

Influence of Electromyogram (EMG) Amplitude Processing in EMG-Torque Estimation

by

Oljeta Bida

A Thesis

Submitted to the Faculty

of the

WORCESTER POLYTECHNIC INSTITUTE

in partial fulfillment of the requirements for the

Degree of Master of Science

in

Electrical Engineering

January 2005

_____

Professor Edward A. Clancy, Thesis Advisor

_____

Professor Donald R. Brown, Comittee Member

_____

Professor David Cyganski, Comittee Member

To my dearest family,
for their selfless sacrifices,
and for the continuous belief in my capabilities
regardless of my weak moments and the obstacles
that we have gone through.

ABSTRACT

A number of studies have investigated the relationship between surface electromyogram (EMG) and torque exerted about a joint. The standard deviation of the recorded EMG signal is defined as the EMG amplitude. The EMG amplitude estimation technique varies with the study from conventional type of processing (i.e. rectification followed by low pass filtering) to further addition of different noise rejection and signal-to-noise ratio improvement stages. Advanced EMG amplitude processors developed recently that incorporate signal whitening and multiple-channel combination have been shown to significantly improve amplitude estimation. The main contribution of this research is a comparison of the performance of EMG-torque estimators with and without these advanced EMG amplitude processors.

The experimental data are taken from fifteen subjects that produced constant-posture, non-fatiguing, force-varying contractions about the elbow while torque and biceps/triceps EMG were recorded. Utilizing system identification techniques, EMG amplitude was related to torque through a zeros-only (finite impulse response, FIR) model. The incorporation of whitening and multiple-channel combination separately reduced EMG-torque errors and their combination provided a cumulative improvement. A 15^{th}-order linear FIR model provided an average estimation error of 6% of maximum voluntary contraction (or 90% of variance accounted for) when EMG amplitudes were obtained using a four-channel, whitened processor. The equivalent single-channel, unwhitened (conventional) processor produced an average error of 8% of maximum voluntary contraction (variance accounted for of 68%).

This study also describes the occurrence of spurious peaks in estimated torque when the torque model is created from data with a sampling rate well above the bandwidth of the torque. This problem is anticipated when the torque data are sampled at the same rate as the EMG data. The problem is resolved by decimating the EMG amplitude prior to relating it to joint torque, in this case to an effective sampling rate of 40.96 Hz.

Keywords: EMG, EMG Amplitude, Torque, EMG-torque Model, Optimal Sampling Rate, System Identification, and Linear Torque Model.

ACKNOWLEDGMENTS

I am deeply thankful to my advisor, Professor Edward Clancy, who initially introduced me to the fascinating field of Electrical Engineering, during my freshman year while taking EE2011. My respect toward him grew as I started to realize that the knowledge gained and the work ethics developed in my introductory class brought me to this point. I feel honored to have had a chance to work with him in this research for my Masters Degree and because of him to have reached so far. Without his guidance and support, the completion of this thesis would not have been possible.

I thank Dr. Denis Rancourt from University of Shebrooke (Canada) for his help throughout the course of this project and for extending his help even beyond this project completion. Heartfelt thanks to my MQP advisor Professor David Cyganski and to Professor Rick Brown for their presence in the research committee and their helpful advice in the project. Also thanks to my lab-mates Karthik and Hongfang for the joyful, kind, and sharing atmosphere created in our lab.

I owe everything I am and I have done to the selfless sacrifice and to the love which my family raised me with. We have been together through many hardships and now it is time to enjoy the fruits of our work. Thanks to my dearest sister Ana for the mutual love and loyal friendship. *"Falenderoj nga thellesia e zemres prinderit e mi te shtrenjte per sakrificen dhe durimin gjate veshtiresive. Nuk mund ta imagjinoni dot mirenjohjen per dashurine, vullnetin, dhe vlerat shpirterore me te cilat me kini rritur duke shpresuar qe nje dite te arrijme te gjitha endrrat e thurura se bashku."*

Thanks to my husband-to-be Eno for being my best friend and for already standing by me for better and for worst. With his continuous love and care, he has encouraged me to work harder to reach our life dreams.

Beyond all and everything, I am thankful to the Almighty God, for answering my prayers, and for always guiding me toward happiness and peace.

TABLE OF CONTENTS

LIST OF FIGURES

LIST OF TABLES

CHAPTER 1. INTRODUCTION

"Electromyography is a seductive muse because it provides easy access to physiological processes that cause the muscle to generate force, produce movement, and accomplish the countless functions that allow us to interact with the world around…To its detriment, electromyography is too easy to use and consequently too easy to abuse."

[Carlo J. De Luca, 1993]

The contraction of muscle fibers generates electrical activity that can be measured by electrodes affixed to the skin surface on top of the muscle group. The recorded spikes of electrical activity are referred to as the electromyogram signal or "raw" EMG. The surface EMG signal recorded using large electrodes (e.g., diameter 5 mm) that monitor the activity of multiple muscle fibers can be well modeled as a zero-mean time-varying stochastic process. Motor units are the smallest functional muscle group. It is observed that the standard deviation of the raw EMG signal is monotonically related to the number of the activated motor units and the rate of their activation. This standard deviation is used to approximate the magnitude of the muscular electrical activity referred to as EMG amplitude [Clancy and Hogan, 1997]. EMG amplitude has a variety of applications, such as a control signal for myoelectrical prostheses, ergonomic assessments, biofeedback systems, and it is used to approximate the torque about a joint [De Luca, 1993; Thelen et al., 1994; Gottlieb and Agarwal, 1977; Valero-Cuevas et al., 2003].

1.1. PROJECT MOTIVATION

After obtaining high quality estimates of EMG amplitudes, a common practice is relating them to the tension of individual muscles via mathematical models, even though

there are limitations to this method. The tension produced by individual muscles can not be measured non-invasively, thus there is no direct mechanical method to validate the model predictions. In addition, the existence of cross-talk (defined as the interfering electrical activity from the surrounding muscles) and the inability to measure this effect add to the difficulties of creating this model.

Considering the mentioned limitations, many researchers [Gottlieb and Agarwal, 1977; Clancy and Hogan 1997; Thelen et al., 1994] have focused their efforts on relating the EMG amplitude to the torque about a joint as the next logical and practical alternative. The effect of cross-talk may be automatically canceled or minimized in the case of the torque about the joint [Clancy et al., 2001]. Total net torque about a joint can be easily verified via mechanical measurements. Furthermore, considering co-activation effects on underlying group muscles, the system model performance is evaluated against the net joint torque contribution, rather than the individual ones that are impossible to distinguish.

Over the last few years, there are clear advances in estimating EMG amplitude yet the EMG-torque modeling has not benefited from this progress. If EMG is a useful indicator of the muscular tension, it is necessary to develop accurate means of quantification, both in terms of properly measuring and interpreting EMG and in creating mathematical models relating EMG-torque. Amplitude estimation accuracy influences the performance of EMG-torque models, because torque about a joint (tension exerted in muscles) is the outcome of proper EMG signal interpretation and consequently its careful treatments. The importance of EMG signal processing can not be emphasized enough, since

electromyography is such a powerful and physiologically easily obtained tool, therefore as expressed by De Luca, its misusage can lead to fatal mistakes [De Luca, 1993].

Demonstrating the benefit of utilizing advanced EMG amplitude processing, Clancy and Hogan (1997) showed that the torque estimation error is reduced when using improved EMG amplitude processors. The experiment results were obtained using a linear model to relate EMG amplitude from biceps/triceps to the elbow joint torque in the case of constant-posture and constant-force contractions. Additionally, encouraging results were also obtained in less constrained conditions (slowly varying force), but several trial combinations that lead to unrealistic model performance (considered as model non-convergence) were an obstacle that needed further investigation [Bouchard, 2001]. The result of the previous research inspired the focus of this project: relating the EMG amplitudes from biceps/triceps to the torque about the elbow and proving that better EMG amplitude processing leads to better torque predictions during dynamic experimental tasks (force-varying contractions).

1.2. THESIS CONTRIBUTION

The goal of this project was to demonstrate that the usage of high fidelity processing techniques (inclusion of whitening filters and multiple channels) for EMG amplitudes leads to improvements in the accuracy of estimating torque. To achieve this main objective, it was necessary to develop a model to relate EMG amplitude to torque and compare the model performance, as the EMG amplitude processors were varied among four different types. These four types of processors were obtained using the combination of multiple channel recordings with the addition of adaptive whitening. The four processors created were: single-channel-unwhitened, single-channel-whitened, multiple-

channel-unwhitened, and multiple-channel-whitened. Further accomplishment was to determine the decimation rate required for the data prior to applying them to the system identification algorithms. Decimation solved some model non-convergence problems encountered during prior research [Bouchard, 2001].

In conclusion, there are several important deliverables from the completion of this project work. The first is the model used to relate extension/flexion EMG amplitudes to torque about the elbow. The second is the data pre-processing routine (decimation) required to achieve the maximum performance from the model. Finally, the thorough documentation of the results and the steps achieving them, along with the recommendations for improvements will serve as starting point for future research.

1.3. THESIS CONTENT

The content of this paper is presented in a logical and chronological, order as appropriate in order to explain the process involved in completing the project. CHAPTER 2 provides background information about the EMG signal starting from its recording to amplitude processing techniques, focusing on the adaptive whitening filters as a new step that has revolutionized the existing processing methods. There is also a review of some of the most common system identification models. The chapter ends with a brief review of the literature on EMG-torque modeling techniques. Following the background, CHAPTER 2 is the model design development chapter. It includes all physiological concepts and thoughts that were poured into quantifying the EMG to torque relationship, reaching into the linear (ARX) model used in this project. The model then is solved, describing most of the algebraic steps involved into obtaining a linear least squares error solution.

CHAPTER 4 explains the data collection method and the process of obtaining EMG amplitudes from the four different processors. EMG amplitude estimation, decimation, and truncation are part of a pre-processing routine used prior to system identification. The system identification procedure involves two main steps, training and validation. During training, a coefficient vector is fit to the input data based on the least squares error minimization. Model validation requires utilizing a distinct dataset to estimate the output using the optimal coefficients. The details of the train-test paradigm along with definitions of model performance quantifiers are also explained in this chapter. The subsequent CHAPTER 5 describes the results obtained after following the tests explained in the previous methodology chapter. The chapter includes general observations and hypotheses derived through experimental data interpretation to validate the observations.

Interpretation and the study limitations are discussed in detail in the last chapter (CHAPTER 6). This chapter summarizes the main contribution of this research and it lays out some suggestions for future work, based on the conclusions drawn. Finally, the document ends with the APPENDICES: that includes additional information on the experimental data and some additional plots that were not crucial to the results, but support their interpretations.

CHAPTER 2. PROJECT BACKGROUND

The content of this chapter is intended to provide background information necessary to understand the subsequent sections that describe the specific thesis contribution. The chapter starts with a brief introduction of the physiological raw EMG signal, focusing on the random character of EMG. Then, it continues with a brief description of the techniques used to process the EMG amplitude. At the end, there is a review of achievements in relating the surface EMG amplitude to the torque about a joint following a summary of modeling techniques.

2.1. EMG SIGNAL FUNDAMENTALS

The electromyogram (EMG) is the recording of the electrical activity produced within the muscle fibers. The relation of surface EMG to torque makes EMG an attractive alternative to direct muscle tension measurements, necessary in many physical assessments. However, the complexity of the EMG signal origin has been a barrier for developing a quantitative description of this relation. The EMG signal origin and character is necessary background to understand the difficulty of establishing a relationship between surface EMG and torque. The description in this section is brief and selective; the reader is suggested to review Basmajian and De Luca (1985) for more details.

2.1.1. Electrical Activity Generation

Electrical activity in the muscles arises from the contraction of the muscle fibers, the structure of which is shown in Figure 2.1. Each muscle fiber contains a bunch of

myofibrils (long chains of contractile units). The myofibrils contain long chains of contractile units called sarcomeres, which contribute to the force exerted within the muscles.

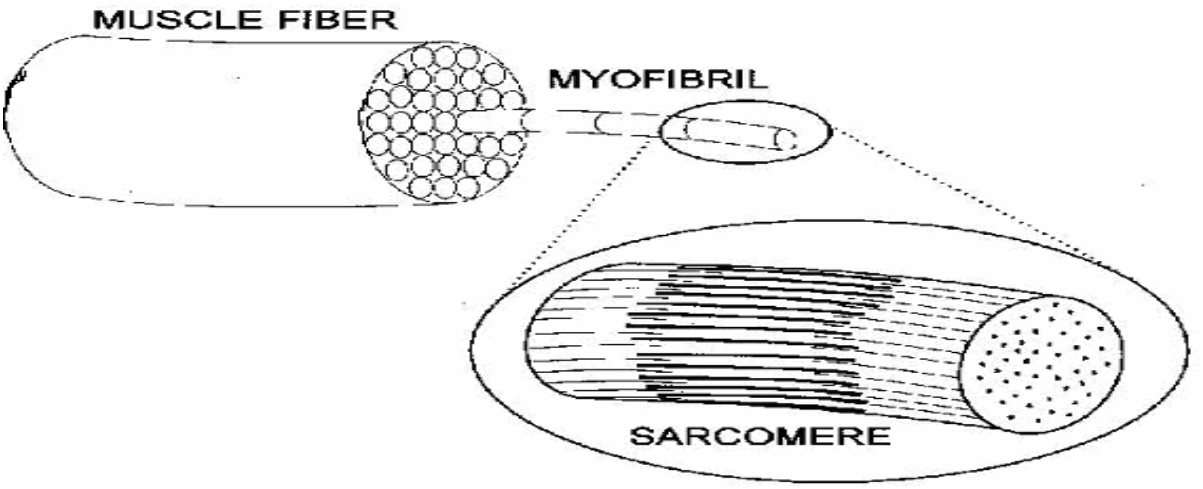

Figure 2.1: Muscle Fibers Composition [Perry and Bekey, 1981]

Each of the myofibrils is chemically activated by local neurons, generating an electrical charge that moves up and down the myofibril, activating the chains of sarcomeres (Figure 2.2). The charge motion generates an electromagnetic field that induces volume conduction, which enables recording of an electrical signal both internally at the muscle and externally at the surface over it. The detected waveform resulting from the depolarization of the wave propagating between the motoneuron and end plate is called the muscle fiber action potential (MAP). MAPs are not commonly seen in the general EMG literature, because they are recorded using microelectrodes, and can not be picked up by the non-invasive surface electrodes.

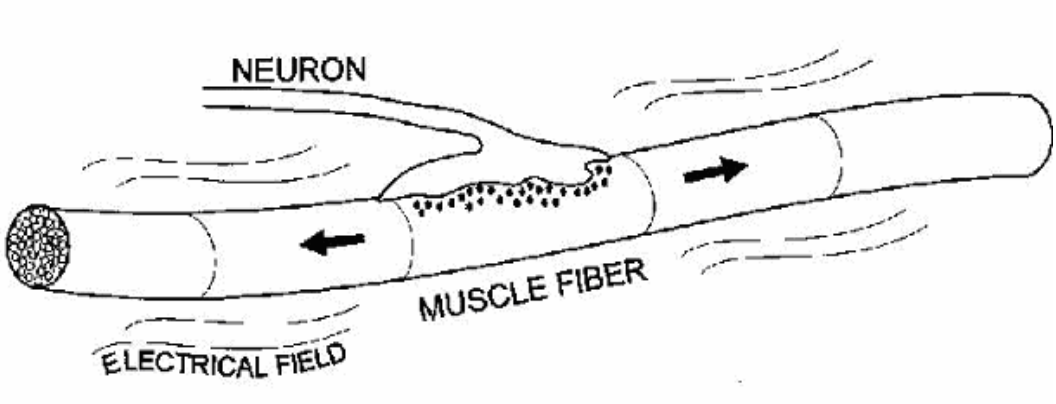

Figure 2.2: Generation of Electric Field in Muscle Fibers [Perry and Bekey, 1981]

The muscle fibers contract in groups that are controlled by the central nervous system via nerve fibers (axons) transmitting the signal to the ending neurons. To simplify analysis and mathematical interpretation of EMG, the smallest controllable functional unit of muscle fibers is defined as a motor unit (MU). The motor unit consists of a *single motoneuron*, its *neuromuscular junction*, and the *muscle fibers* that it excites. The number of the muscle fibers contained in a MU varies with the size of the muscle within which a MU belongs. Smaller muscles have MUs that contain 3-10 myofibrils, while larger ones contain up to 2000 myofibrils. It is important to emphasize the similar structure of the muscles, regardless of the scaling on the size and the number of myofibrils [Perry and Bekey, 1981; Lamb and Hobart, 1998].

2.1.2. Origin and Character of EMG

Microelectrodes on the cell surface are not the only way to measure motor action potentials. The living tissues act as volume conductors, therefore a potential at the motoneuron source is spread away via ion movements throughout the entire unit volume. Applying the same principles of conduction described above, the action potential

propagates along the motoneuron to the endplate of the muscle fibers (Figure 2.3). The electrical potential surrounding the muscle fibers changes, because the geometry of the conducting volume changes. Therefore, the conduction times of the muscle fibers in a motor unit are different. The spatio-temporal summation of the individual myofibril action potentials recorded by the electrode is called a motor unit action potential (MUAP). Figure 2.3 represents the motor unit action potential as the superposition of MUs generated by each of the myofibrils. Each muscle fiber within the MU (on the left of the figure) contributes to the surface potential (on the right of the figure). [Basmajian and De Luca, 1985].

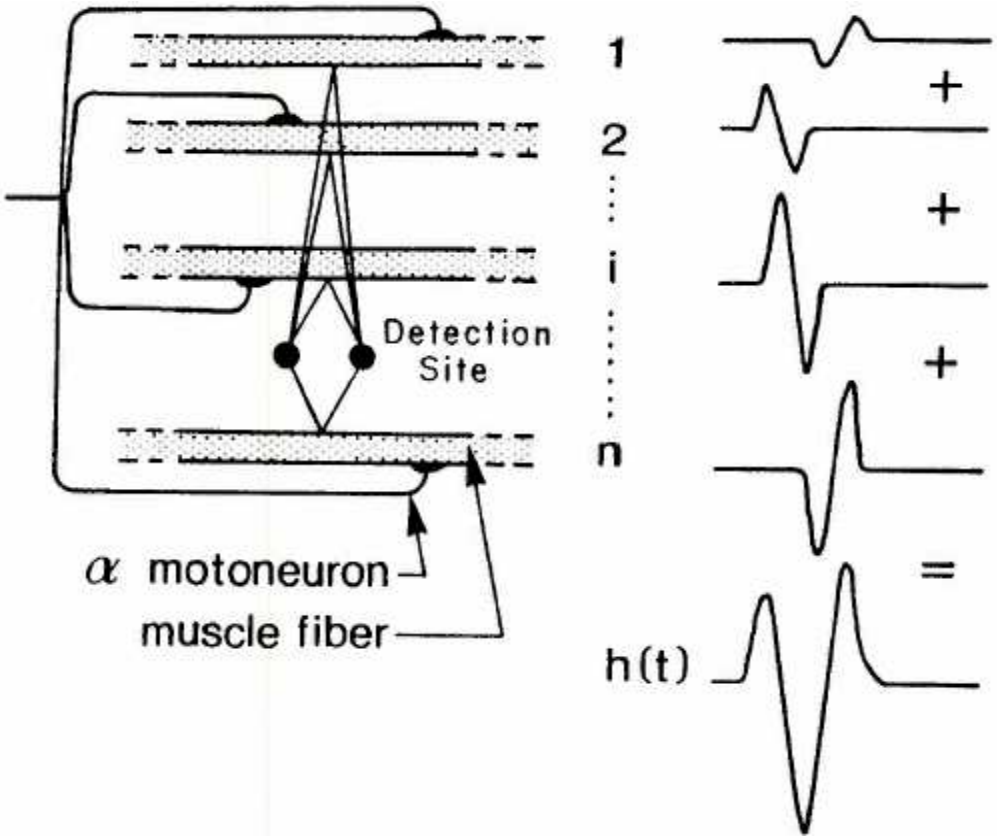

Figure 2.3: Observed Motor Unit Action Potential, MUAP [Basmajian and De Luca, 1985].

The recorded MUAP is an attenuated version of the action potential generated in the muscle fibers because of the filtering effect that is due to the transmission line between the motoneuron and electrode. In particular, the tissue acts as a low pass filter with a cutoff frequency proportional to the distance of the electrode to the signal source [Lindstrom and Magnusson, 1977]. Usually, the individual MUAP is recorded using fine wire electrodes, although under certain conditions surface electrodes can be used. The duration of the MUAPs can vary from a few milliseconds to 14 ms, and their amplitudes vary from microvolt ranges to a maximum of 5 mV. Typical surface EMG electrodes are used to record the myoelectric activity of the skeletal muscle as a whole, rather than individual MUAPs. Generally, the pick-up area of an electrode includes more than one motor unit, because muscle fibers of different motor units are mixed throughout the entire muscle [Lamb and Hobart, 1992].

The MUAP is the response of the motor unit MU to a single motoneuron excitation. If the stimulus is modeled as an impulse dirac function, $\delta(t)$, then the MUAP is considered the impulse response $h(t)$. The repetitive sequence of stimulations to the motor units results into a series of impulse responses referred to as the motor unit action potential train (MUAPT). Each of the motor unit responses to the impulse train is independent from the sequence and the total series response has a random character. Therefore, the superposition of the MUAPTs is the physiological EMG signal and can be modeled as stochastic process (sum of independent random variables).

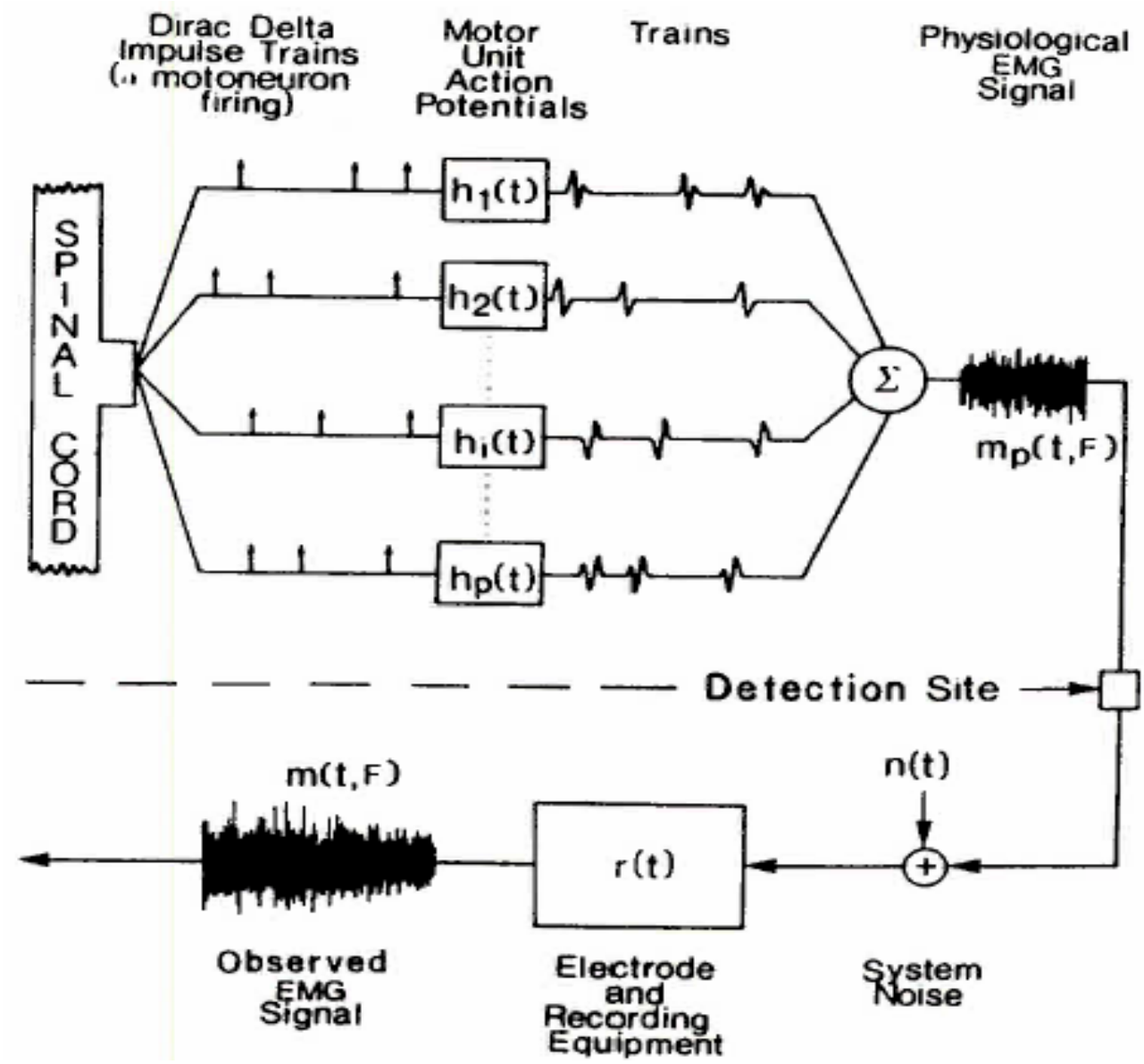

Figure 2.4: EMG Signal Origin Block Diagram [Basmajian and De Luca, 1985]

A schematic representation of the EMG generation is shown in Figure 2.4. The symbol $m_p(t, F)$, myoelectric signal as a function of time (t) and the number of firings (F), represents the physiological EMG and it is not recordable or measured. The detected EMG signal that is utilized in the research is the observed signal m(t, F) that is

contaminated with electronic noise (almost white) and has lost some of the high frequency components due to the filtering effects at the electrodes [De Luca, 1993].

To conclude, considering the EMG signal as a time varying stochastic process gives the possibility to model it as a zero-mean Gaussian distribution, because EMG is the sum of a large number of MUAPs [Papoulis, 2002]. This random character of the EMG signal enables the later described approximation of EMG amplitude as the square root of the detected signal's variance. In addition, the recorded EMG signal is dependent on the type, geometry, and position of the recording electrodes. The depolarization wave also causes chemical changes that result in a mechanical twitch, which is slower than the electrical response, and delayed by 50-100 msec. This mutual relation of EMG and mechanical activity to the MUAPs inspires the establishment of an EMG-torque relationship that will be discussed in detail in the upcoming chapters.

2.1.3. Factors that Effect EMG Signal

There are many factors identified in the research as having a great influence on EMG interpretation. Even though they all are important, a common practice among researchers has been to focus on the effects that have the most impact on the application for which the EMG signal is used [DeLuca, 1993; Farina, Merletti, and Enoka, 2004; Perry and Bekey, 1981; Lamb and Hobart, 1992]. This section also will follow the same rule, and briefly describe some of the factors that directly effect the EMG signal interpretation and analysis when estimating torque. Quantifying the factors that effect EMG signals is a complex task, because there is not enough information to validate the assumptions. Considering the varieties in the structure of electrodes and living tissues, it also is impossible to generalize the observations over all subjects and cases.

De Luca (1993) categorizes the factors that effect EMG signal and force into three groups: causative, intermediate and deterministic factors. The causative factors are the basis of EMG signal and they are both intrinsic and extrinsic. The extrinsic factors are related to the electrode structure and its placement on the skin overlying the muscle. Such instances include the electrode configuration, location, and the orientation of detection surfaces relative to the muscle fibers. On the other hand, the intrinsic causative factors are related to the physiological, anatomical and biochemical character of EMG signals. These factors can not be controlled, but their knowledge and understanding help with the accuracy of EMG interpretation. The causative intrinsic factors include the number of active MUs at the time, the pH level in the muscle fibers, the blood flow, and geometry of the fibers. The intermediate factors (i.e. cross-talk, conduction volume and velocity, superposition, etc.) are the effects that are influenced by the causative factors and in consequence they influence the deterministic factors (i.e. number of MUs activated, MU firing rate, MUAP shape and duration, etc.). The amount of the effect that the deterministic and the intermediate factors have on EMG is an application-based evaluation.

Table 2.1 from Farina et al. (2004) represents a summary of the known effects to EMG interpretation. The presence of subcutaneous fatty tissues becomes a significant factor, because the loss of the high frequency components reduces the spectrum of the EMG signal. Besides the stability of the position of the electrodes and the stability of the MU firing rate, the issue of crosstalk is always present. Crosstalk is defined as the interference pattern recorded from a distant muscle when the electrodes are intended to monitor another muscle. Crosstalk is an issue that can be misleading when EMG is

explained by the properties of volume conduction. Simulation and analyses have shown that the crosstalk can neither be measured nor eliminated with the existing technology. Therefore, it should be recognized while utilizing EMG to estimate muscle forces [Farina, Merletti and Enoka, 2004].

Table 2.1: Factors that Influence Surface EMG [Farina, Merletti, and Enoka, 2004]

Non-physiological	
Anatomic	**Shape of the volume conductor**
	Thickness of the subcutaneous tissue layers
	Distribution of the MUs territories in the muscle
	Size of the motor unit territories
	Distribution and the number of fibers in the MU territories
	Length of the fibers
	Spread of the endplates and tendon junction within MUs
	Spread of the innervations zones and tendon regions among MUs
	Presence of more than one pinnation angle
Detection System	**Skin electrode contact (impedance or noise)**
	Spatial filter for signal detection
	Inter-electrode distance
	Electrode size and shape
	Inclination of the detection system relative to the fiber orientation
Geometrical	**Location of the electrodes over the muscle**
	Muscle fiber shortening
Physical	**Shift of the muscle relative to the detection system**
	Conductivities of the tissues
Physiological	**Amount of the crosstalk from the nearby muscles**
Fiber membrane properties	**Average muscle fiber conduction velocity**
	Distribution of the MU conduction velocities
	Distribution of the conduction velocities within in MUs
	Shape of the intracellular action potential
Motor unit properties	**Number of recruited MUs**
	Distribution of motor unit discharge rates
	Statistics and coefficient of variation for discharge rate
	MU synchronization

2.2. SURFACE EMG AMPLITUDE ESTIMATION TECHNIQUES

If the EMG amplitude is defined as the standard deviation of the raw EMG signal, then it can be estimated by applying standard statistical techniques [Clancy and Hogan, 1997]. Since raw EMG is a stochastic process in nature, its statistical processing can be used for predictive purposes. The estimation of the EMG amplitude has been refined and improved since the early EMG amplitude developed from a simple rectifier and low-pass filtering [Imnan et al., 1952]. The state of art EMG amplitude processing includes six stages that will be discussed separately after a brief presentation of the complete process.

2.2.1. Standard EMG Amplitude Estimation

The most common technique of detection for EMG amplitude is the rectification process followed by a smoothing step. According to Hof and Van Den Berg (1981), the recorded EMG signal is described as the product of a zero-mean stochastic process with the time-varying EMG intensity. Therefore the intensity of the EMG signal (EMG amplitude) can be obtained by proper rectification and smoothing [Hof and Van Den Berg, 1981]. The early researchers in the field studied and utilized non-linear analog circuits, such as a full wave rectifier and a low pass filter made of simple passive components (resistors and capacitors), to detect the signal [Bigland and Lippold, 1954]. This method eventually led to the use of the statistical moving average mean absolute value (MAV) and the moving average root mean square (RMS).

Moving Average Mean Absolute Value: $$MAV_t = \frac{1}{N}\sum_{i=t-N+1}^{t}|x_i| \qquad (2.1)$$

Moving Average Root Mean Square: $$RMS_t = \sqrt{\frac{1}{N}\sum_{i=t-N+1}^{t}x_i^2} \qquad (2.2)$$

where in both expressions N is the number of samples in each smoothing window of the moving average filter; t is the time at which this interval starts; and x_i is the signal being smoothed in the time-domain.

EMG amplitude can also be computed in software using either one of the above formulae. The amplitude estimates found using RMS and MAV calculations exhibit very similar performance. However, the MAV method has been initially used more than the RMS, because of the lesser amount of time necessary for computations. Currently, the computation time is not as problematic especially when processing is performed offline.

The process of detection is followed by smoothing and relinearization. The method of accomplishing the two last steps differs between RMS and MAV. In the case of RMS, the detection of the signal is achieved by squaring all the terms. The resulted squared terms are smoothed by taking their average and then relinearized by taking the square root of the mean. The detection for the MAV method is done by taking the absolute value of the terms. The result is smoothed by taking the average of these terms. In this case, there is no need to relinearize.

2.2.2. Advanced EMG Amplitude Estimation

The EMG signal processing is a crucial factor in the way that EMG amplitude is interpreted and used in different applications. Therefore, specifying and understanding the steps involved in the processing technique is extremely important. The estimator has evolved from the use of a simple rectification and a low-pass filter. An advanced EMG amplitude estimator consists of the following six stages (Figure 2.5):

1. *Noise rejection filter*
2. *Adaptive whitening*
3. *Multiple Channel Combination and Gain Normalization*

4. *Rectification and Demodulation*
5. *Smoothing*
6. *Relinarization*

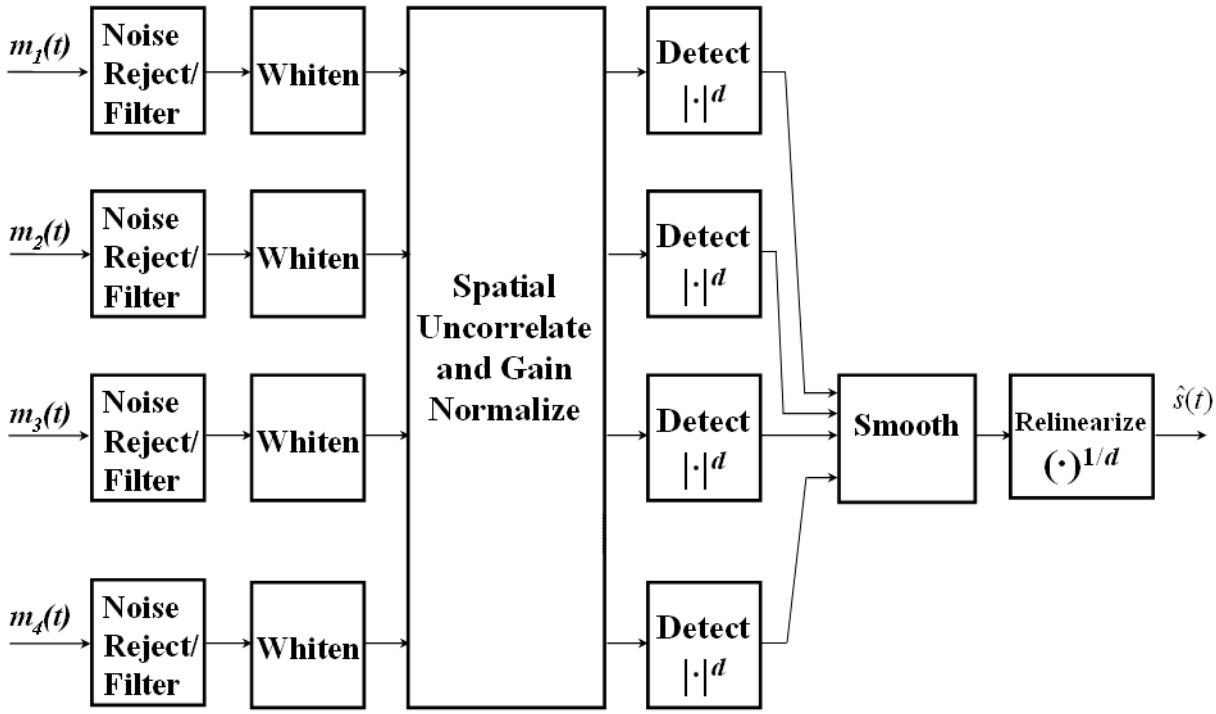

Figure 2.5: Six Stages Multi-Chan-Whit EMGamp Processor [Clancy et al., 2001]

In the above figure, inputs m_k (k = 1-4) are the recorded signals from the surface electrodes placed on top of each of the muscle groups. The output $\hat{s}(t)$ is the estimated EMG amplitude (EMGamp). The pictorial presentation of the signal transformation for each of the channels is given in Figure 2.6.

Each of the surface EMG signal m_k is transformed to the EMG amplitude $\hat{s}_k$ after passing through all the stages of the processor. In the first stage, motion artifact is attenuated with a high-pass filter. In the second stage, the signal is whitened. The adaptive whitening has demonstrated better performance for low-amplitude levels. Stage three rectifies the signal and then raises it to a power to make it nonlinear. In stage four, the demodulated samples are averaged (smoothed). In stage five, the signal is

relinearized by raising it to the inverse of the power applied previously. During the "Detect" and "Relinearize" stages, d=1 for MAV and d=2 for RMS.

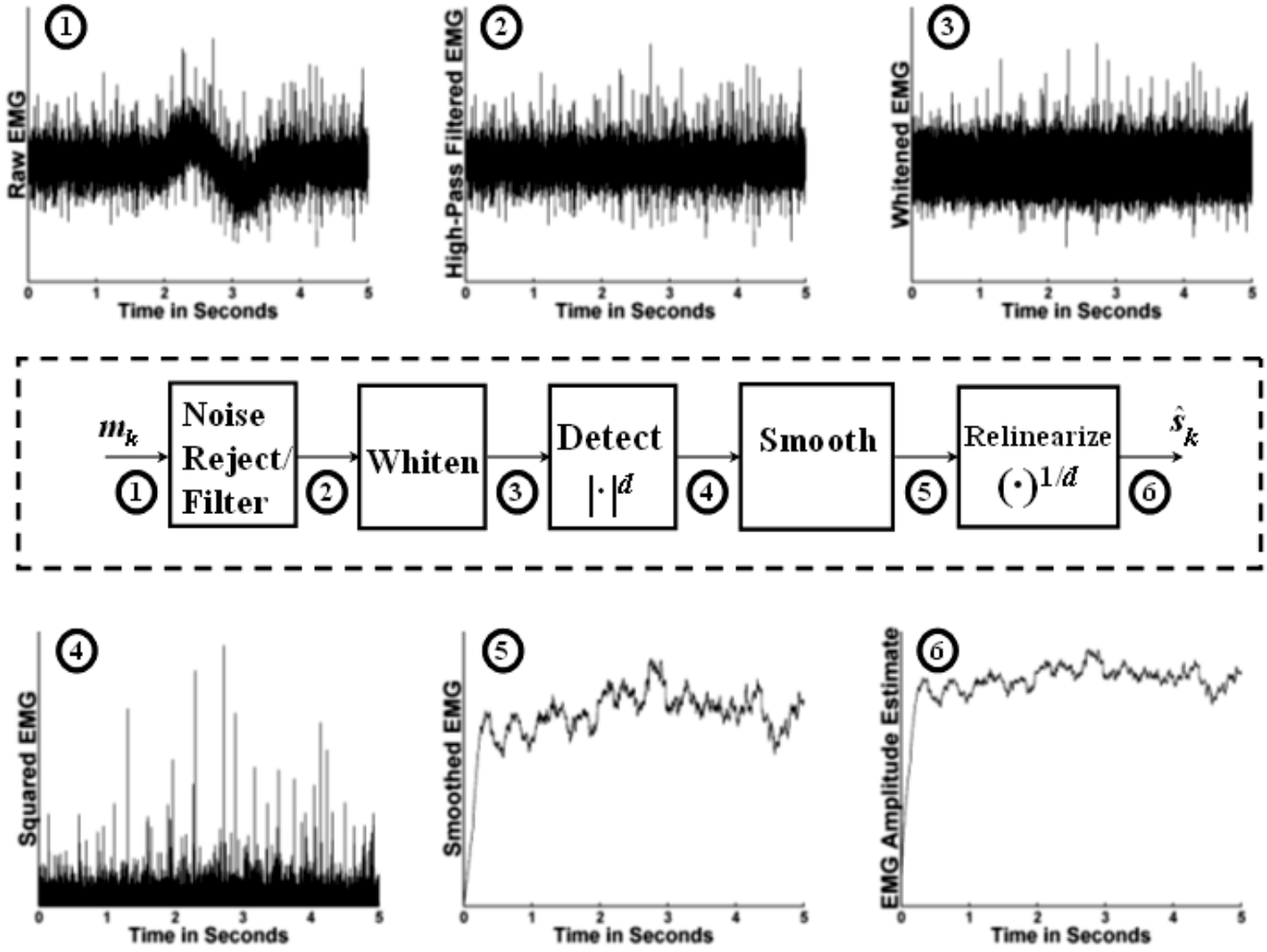

Figure 2.6: Single-Chan-Whit process for EMGamp estimation [Clancy et al., 2004]

The smoothing step is omitted when the EMG amplitude obtained is used to estimate torque. Additional detail of these steps is given in the following sections.

2.2.3. Noise Rejection Filters

High pass filters, prior to RMS and MAV, are used to eliminate the noise from motion artifact. The power density of motion artifact is mostly below 20 Hz; therefore, a

high-pass filter with cutoff frequency between 10-20 Hz is sufficient to reduce/eliminate these effects. Cutoff frequencies greater than 20 Hz can cause loss of EMG signal, considering that the roll-off of the real filters can coincide with the median frequency of the EMG signal, especially during fatigue [Clancy, Morin, and Merletti, 2002]. The high pass filter can be analog incorporated into the hardware instrumentation and/or digital implemented in software. The advantage of using digital filters is the ease of implementing high order filters to achieve sharp roll-off and eliminate more of the noise power ensuring that the loss of useful information is minimal. In some cases, analog filters are used in addition to digital filters to prevent saturation caused if the EMG signal is corrupted by large amplitude motion artifact.

2.2.4. Adaptive Whitening

The whitening step is recently included in EMG signal processing software algorithms. The term whitening originates from the power of the white light spectrum spreading out uniformly over all frequencies. Whitening an EMG signal is the process of decorrelating the neighboring samples in the time domain. Doing so, the statistical bandwidth increases therefore the approximation of standard deviation is more accurate [Bendat and Piersol, 1986]. The adaptive whitening removes the additive noise described in the physiological model of EMG created by Clancy and Farry (2000) presented in Figure 2.7.

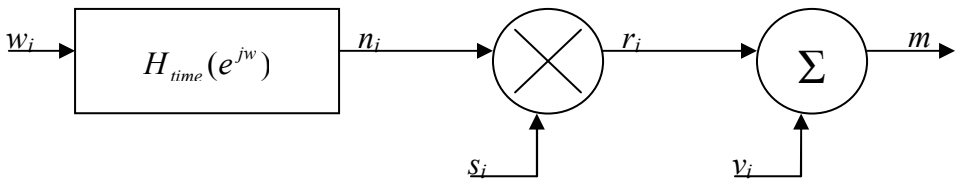

Figure 2.7: Model of EMG used for adaptive whitening filters [Clancy and Farry, 2000]

A more detailed description of the model and the math behind it can be found in the original source. Briefly, the signal w_i is a zero mean Gaussian random process of unit variance that serves as a start for modeling the EMG. This signal is passed through a shaping filter, H_{time} that creates the low-pass effect of the tissues and skin layers on real EMG signal while still maintaining unit standard deviation. The output (n_i) is then multiplied by the amplitude of EMG (s_i) resulting to the noise-free EMG (r_i). The signal v_i is a zero-mean random process representing additive electronic noise and random noise from the electrode-skin interface that is summed with r_i to complete the model of the measured surface EMG, m_i. Recalling the physiological description of EMG in the previous section, this model is consistent with the character of the raw EMG in Figure 2.4.

The shape of adaptive whitening filters is formed based on the power spectral density (PSD) of the noiseless signal and the additive noise. Briefly, the shape of the original whitening filter is the inverse square root of the PSD taken from the true EMG signal. The adaptive whitening involves incorporating a noise attenuation stage that operates based on the relative power of the signal over the existing noise. Adaptive whitening is necessary, because it is observed that the noise exhibits a larger relative

magnitude during low level contractions, where the relative EMG intensity is lower. The time duration of the whitening filter is short; hence, the EMG amplitude remains essentially constant during that period, making the adaptive whitening process quasi-stationary [Clancy and Bouchard, 2001].

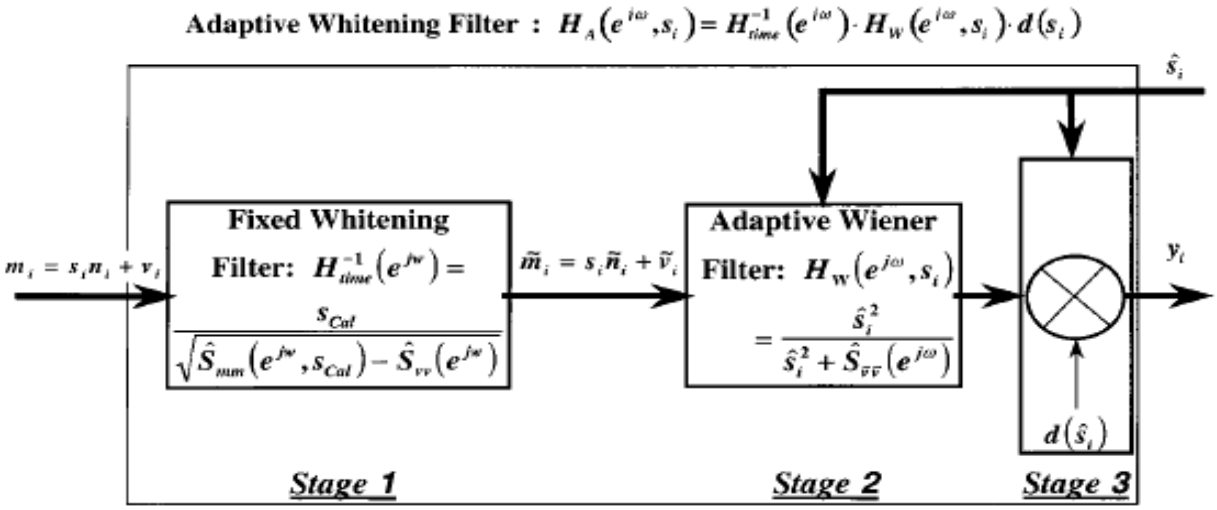

Figure 2.8: Adaptive whitening of EMGamp estimation [Clancy and Farry, 2000]

The whitening process proposed by Clancy and Farry (2000) includes three stages used to improve amplitude estimation (Figure 2.8). Without including the details (they can be found in the mentioned source) the first stage of this process whitens the noiseless EMG amplitude s_i, but also a filtered version of the additive independent noise v_i. The second stage optimally estimates the noise-free whitened signal $\overline{m}_i$ by adaptively removing the noise through a Wiener filter. The third stage applies an adaptive gain determined based on the transformations of EMG signal from the two previous stages. This step is used to maintain the variance of the EMG signal throughout the complete whitening stage [Clancy and Farry, 2000].

2.2.5. Multiple Channel Combination and Gain Normalization

This step involves the combination of EMG recordings obtained from several electrodes placed adjacent to each other, on the skin overlying the same muscle. The reason for the combination of multiple channels is that the SNR improves with the increase in the volume of muscles recorded. Since the gain and the distance from the muscle differ from electrode to electrode, the combination of the recordings is followed by the gain normalization process. This ensures equal contribution from each of the recordings, and can be considered as decorrelation of the signal spatially. Research has shown that using several electrodes for measuring the EMG from a muscle results in more accurate EMG amplitude estimation. SNR performance improvements of up to 91% have been observed using multiple channels, as compared to the results from a single channel processing [Hogan and Mann, 1980b]. There are also some disadvantages to the multiple electrode recording combination including that the chance of defects that may arise due to noise, shorted electrodes, etc. is increased with the number of channels [Hogan and Mann, 1980a].

2.3. BIOMECHANICAL SYSTEM MODELING TECHNIQUES

System identification is a study of the dynamics and physical behavior of systems under external disturbances. Specifically, it is a set of standardized guides on building system mathematical models based on observations made on system reactions. The external data that can be manipulated and measured by the user are referred to as inputs and others as disturbances, even though most of the time their difference does not affect the modeling process. The measured/observed response of the system is referred to as its

output. This section gives a brief description of the system identification. Detailed reference of the models and system identification techniques are found in Ljung (1999).

The dependence of the recorded EMG signal and muscle tension on mutual physiological factors inspires on-going research work to develop mathematical models relating EMG to torque. The experimental studies have explored both linear and nonlinear models to achieve better accuracy. Some researchers have even built complex models that describe the details of muscles, however little or no improvement is seen in doing so. Keeping in mind the ultimate goal of this research, this section also illustrates the forgoing theory of mathematical modeling with some EMG-torque examples found in the literature.

2.3.1. Overview of Modeling Techniques

Modeling of the complex relationship between muscular activity and torque has been approached in two different methods; a priori (*morphological*) and a posteriori (*black box*) type of modeling techniques [Westwick, 1995]. The morphological modeling technique involves designing a model based on the physical characteristics of the system. The parameters are flexible and well adapted to the system itself. The drawback of this method is the large number of parameters that result in a high level of complexity. Additionally, it requires a thorough understanding of the system structure, while most of the times, the system is unknown and it is considered as a *black box* (Figure 2.9). The black box type of modeling is referred to as system identification, and it is used to obtain a relationship between inputs and outputs, rather than determining the structure of the system. Although this modeling technique is more practical than the first one, the results require careful interpretation and validation with the physical concepts.

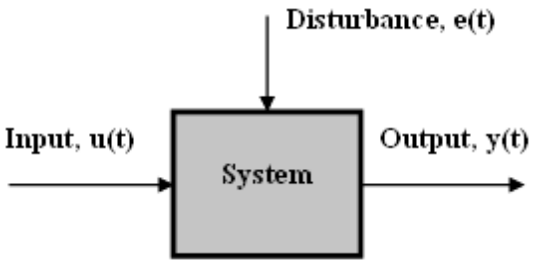

Figure 2.9: System Identification Problem (black-box type of modeling)

The construction of a model via system identification commonly involves three steps. The first step is input/output data collection, which is mostly completed through prior experiments. The second stage is narrowing the model choice to several that fit the system physical capabilities. The last step is model validation, which involves performance error measures. If this last step fails to achieve the error requirements, than the steps are repeated until the desired results are obtained. The data collection process is explained in detail in another chapter, the following sections describe basics of system identification standard models. The types of models described in this study are linear time invariant. Even though these types of systems are limited, the theory developed through them can be used to approximate real systems.

2.3.2. Parametric System Identification

The parametric model is a set of differential or difference equations that describe the operation of the system in terms of inputs and outputs. These equations also include a number of parameters that can be varied to alter the behavior of the model. The values of the parameters are numerically estimated to give the best agreement between the experimentally measured output and the model estimated output. The matching criterion is usually the minimization of the squared error, where error is defined as the difference between the measured and predicted outputs.

Parametric system identification is basically a simplification of general standard equations for dynamic systems. Figure 2.10 shows a general block diagram of a dynamic system. Although many are tempted to use a large number of parameters to describe the system, the number of parameters to identify should be small. The accuracy of coefficients estimation decreases with the number of the parameters to be estimated [Ljung, 1999].

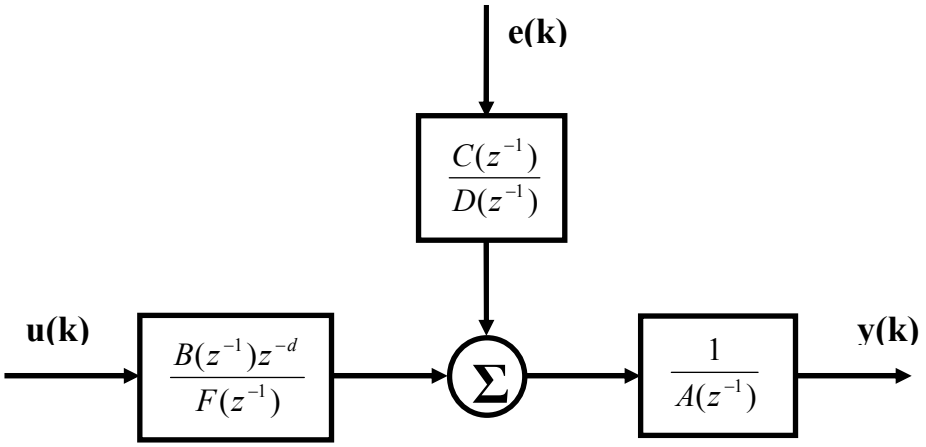

Figure 2.10: Generic Dynamic System Block Diagram (discrete time signals)

The general equation (Z-transform) for the dynamic system is:

$$A(z^{-1})y(k) = \frac{B(z^{-1})z^{-d}}{F(z^{-1})}u(k) + \frac{C(z^{-1})}{D(z^{-1})}e(k) \qquad (2.3)$$

where,

$$A(z^{-1}) = 1 + a_1 z^{-1} + \ldots + a_{na}z^{-na}$$
$$B(z^{-1}) = \quad b_1 z^{-1} + \ldots + b_{nb}z^{-nb}$$
$$C(z^{-1}) = 1 + c_1 z^{-1} + \ldots + c_{nc}z^{-nc}$$
$$D(z^{-1}) = 1 + d_1 z^{-1} + \ldots + d_{nd}z^{-nd}$$
$$F(z^{-1}) = 1 + f_1 z^{-1} + \ldots + f_{nf}z^{-nf}$$

The polynomials represent the components used to find the transfer functions (eq. 2.4) derived from the state space equation of the system behavior. The shift operator z^{-1} is consistent with the z-transform and the negative power represents the right shift in sample-time. In equation 2.3 the term z^{-d} next to coefficient matrix [B] represents the time lag between input and output which means that some leading coefficients of [B] are zero when there is a delay in the system. The order of the polynomials is described by *na, nb, nc, nd* and *nf*. The values of these variables are determined in the process of the system identification, to better match the behavior of the system. If both sides of the equation are divided by the feedback term $A(z^{-1})$, then:

$$y(k) = \frac{B(z^{-1})z^{-d}}{F(z^{-1})A(z^{-1})}u(k) + \frac{C(z^{-1})}{D(z^{-1})A(z^{-1})}e(k) \qquad (2.4)$$

where the input terms next to *u(k)* can be grouped to form the transfer function $G(z^{-1})$ and disturbance terms next to *e(k)* form $H(z^{-1})$. In other words, $G(z^{-1})$ and $H(z^{-1})$ are the transformations of the inputs and disturbances, respectively to obtain the output [Ljung, 1999 Chapter 4].

Table 2.2: Common Black-Box Models, Simplification of General Expression

POLYNOMIALS USED	NAME OF THE MODEL
$B(z^{-1})$	**FIR** – Finite Impulse Response ($n_a = 0$)
$A(z^{-1})$; $B(z^{-1})$	**ARX** – Auto Regressive with eXogenous input
$A(z^{-1})$; $B(z^{-1})$; $C(z^{-1})$	**ARMAX -** Auto Regressive Moving Average with eXogenous output
$A(z^{-1})$; $C(z^{-1})$	**ARMA -** Auto Regressive Moving Average
$A(z^{-1})$; $B(z^{-1})$; $D(z^{-1})$	**ARARX -** Auto Regressive Auto Regressive with eXogenous output
$A(z^{-1})$; $B(z^{-1})$; $C(z^{-1})$; $D(z^{-1})$	**ARARMAX –** combination of ARARX with Moving Average
$B(z^{-1})$; $F(z^{-1})$	**OE -** Output Error
$B(z^{-1})$; $F(z^{-1})$; $C(z^{-1})$; $D(z^{-1})$	**BJ –** Box Jenkins

Simplifying the general equation 2.3 or 2.4, there are several types of standard models that can be developed. Table 2.2 summarizes the special case of a *priori* type of modeling techniques. System identification has no restriction on the number of inputs and outputs to the model. The common use of single/multiple input and output systems has created a specific nomenclature for each of the cases.

- SISO – Single Input, Single Output
- MISO – Multiple Inputs, Single Output
- SIMO – Single Input, Multiple Outputs
- MIMO – Multiple Inputs, Multiple Outputs

The system identification literature describes the solutions and techniques for the single input, single output models (SISO); however, superposition enables the use of the techniques for any case.

2.3.3. EMG-Torque Relationship Modeling

There are many applications that the tension exerted by the muscle group during the various activities is useful, however direct measurements are unnatural, invasive, expensive, and they may also not be possible presently. The assumption of torque being related to the nervous excitation of the individual muscle or the muscle group, relates torque to the magnitude of electrical muscle activity (EMG signal). A relation between EMG and torque simplifies the situation, because EMG is readily obtained by either surface or wire electrodes depending upon whether the muscle group or individual muscle measurements are needed [Perry and Bekey, 1981]. Although many studies have made a great impact in the EMG field, there is no consensus on a standardized set of

models that relate a specific muscle (muscle group) to tension (torque). In addition, the progress in obtaining EMG amplitudes is not yet incorporated into the existing models.

The development of generic prediction models has been less successful, perhaps due to variations in muscle composition. However, different procedures used to record and analyze EMG also need to be considered when determining the relationship between muscular forces and the EMG signal. Several investigators have agreed that it is necessary to incorporate the control strategy for the muscles being investigated, including: the force generation rate, joint angle, muscle length, and muscular co-activation [Solomonow et al, 1990]. It is also determined that changes in recording procedures, including variations in electrode placement, recording configuration and limb position, significantly alter the EMG-torque relationship of the biceps and triceps brachii [Woods and Bigland-Ritchie, 1983].

The interaction of muscles during contractions must be accounted for during analyses. Principal components have been used to minimize the effects of cross-talk, the overlapping affects of independent variables, but generalization may not be possible due to the large number of assumptions and originality of the situations examined [Hughes and Chaffin, 1997]. In general, predicting torque is difficult because so many factors can influence the resulting exertion. The muscle being investigated, procedures implemented, and the form of the force-EMG relationship are vital components for accurately determining force levels. Various approaches have utilized relatively simple models under controlled conditions to determine the torque produced by different muscles groups about different joints.

Studies of the relationship between surface EMG and force have found that there exist both linear and non-linear relationships. Woods and Bigland-Ritchie (1983) investigated the degree of linearity in the torque to EMG relationship and found that linearity existed for muscles such as the adductor pollicis and soleus. They have also found that other muscles, such as the biceps and triceps, behaved non-linearly from 0-30% MVC (maximum voluntary contraction), and then linearly above this range. On the other side, Moritani and DeVries (1978) determined that a linear relationship existed between the electrical muscle activity of the biceps brachii and the muscular tensions produced during exertions. Others have concluded that surface EMG, after processing using rectification and integration, varies linearly with tension generated at a constant muscle length or during contractions with constant velocity [Milner-Brown and Stein, 1975].

Characteristics of the muscle of interest may also influence the EMG to torque relationship. Muscles of uniform fiber composition exhibit a linear relationship while a random non-even composition of fibers behaves more nonlinearly [Woods and Bigland-Ritchie, 1983]. The main fiber type can also influence the linearity with slow twitch muscles behaving more linearly as compared to the non-linear characteristics of fast twitch fibers [Zuniga and Simons, 1969]. Furthermore, the muscles display nonlinear behavior at lower torque levels due to selective recruitment of motor units at different distances from the electrodes. In addition, the dependence on frequency coding (the frequency of the incoming action potentials) for force modulation in the muscles results in linearity while muscles such as the bicep brachii recruit throughout the total range of

force and behave nonlinearly, with the discontinuity at approximately 30% of the maximum voluntary contraction [Woods and Bigland-Ritchie, 1983].

The degree of linearity is dependent on the muscle being investigated, but other factors must be also considered. Milner-Brown and Stein (1975) suggest sampling bias, synchronization, and tension non-linearity also influence the behavior of EMG to torque relationship. Frequency coding has been shown to increase the linearity [Ray and Guha, 1983], whereas tension, length, and velocity characteristics within muscles are nonlinearities that affect the overall relationship [Perry and Bekey, 1981]. Moreover, Zuniga and Simons (1969) determined that there is a nonlinear relationship between averaged EMG potential and muscle tension. In addition to muscle characteristics, the electrode arrangement, type of measurement, fatigue, and level of physical conditioning level may influence the apparent EMG to torque relationship [Zuniga and Simons, 1969].

Recent advances in the research field have demonstrated that linear models can predict shoulder forces during isometric contractions [Laursen et al., 1998]. Additionally, Milner-Brown and Stein (1975) concluded that there was a simple linear relationship between surface EMG and force within the first dorsal interosseus muscle of the hand. However, on the other side, Woods and Bigland-Ritchie (1983) have found that under isometric conditions, the relationship between integrated, smoothed, or rectified EMG and muscle force depends on the physiological characteristics of the muscle. If the muscle mechanics are known, they can be incorporated into a *Hill-type* model that can be used to predict muscle forces [Dowling, 1997]. Linear algebraic equations may not suffice when attempting to explain dynamic situations. The velocity of contractions and the tension produced can be related using Hill's hyperbolic equation

[Perry and Bekey, 1981]. All the above show that the degree of linearity depends on the muscle being investigated, many muscles seem to exhibit a linear relationship between force and EMG, but nonlinear models seem to capture more of the physiological behavior. The usage of linear or nonlinear model depends on the focus of the research work and it is really a matter of perspective of the researchers.

Although clear progress has not been made toward development of generic models, some of the models developed for specific cases have made impact in the field. Armstrong et al. (1982) used rectified EMG signals of the forearm flexor muscles to predict the finger forces produced during tasks involving pinching, grasping and pressing. Grant et al. (1994) predicted grip force from EMG measures and ratings of perceived exertions, and reported that as much as 74% of the variation could be explained. Sommerich et al. (1998) studied typing tasks in an attempt to determine a dose-response relationship for general hand intensive tasks and create generic biomechanical assessments. Buchanan et al. (1993) used surface EMG and anatomical parameters to estimate isometric muscle forces about the wrist using an EMG coefficient method. Although there are limitations with this model, including the lack of repeatability and restriction to "static isometric conditions," torque at the wrist could be estimated with coefficients of variation less than 10%.

Several studies have examined muscle torques produced about the elbow. A multi-channel surface EMG approach by Clancy and Hogan (1997) was used to develop a third order polynomial algebraic relation with an estimation error of approximately 3% to predict torques about the elbow. Furthermore, a model created by Wyss and Pollak (1984) approximated muscle forces about the elbow with 10% error. The EMG-torque

relationship of abdominal muscles required quadratic regression but still did not account for all of the variation around a linear regression line [Stokes et al., 1989]. Extensive work has been conducted on the lumbar musculature during static and dynamic situations with EMG based models being in the focus [Hughes et al., 1994; McGill, 1992; Nussbaum et al., 1995].

In summary, there is a substantial amount of work investigating surface EMG to torque models which confirms the importance of utilizing EMG as a physiologically powerful tool. The above experimental studies are not constrained only to static conditions, individual progress has been made establishing both linear and nonlinear relationships for quasi-isotonic (slowly force varying) and even extending to fully dynamic conditions. While the accomplishments have made an impact in the field, there are clear problems that still exist in some of these studies. First, most of the earlier (more than two decades ago) investigators assumed that the antagonist muscle can be safely neglected, since the mechanical activities of agonist and antagonist muscles are considered independent from each other. Secondly, even though calibration is a common practice nowadays, some researchers neglect the importance of it while some others go beyond and suggest calibrating to each subject separately [Hasan and Enoka, 1985].

The most relevant factor that should remain from this review is the necessity for a method to obtain accurate torque estimation. There is no consensus on the degree of linearity, because the findings are influenced by many factors, such as the dynamic range, the level of the force contraction, and the size of the muscles. The level of the details and the type (physiological or black-box) on the various EMG-torque models is also relative to the focus of the study and it is driven by the main objective, improving the accuracy of

torque predictions. Although the same objective is intended, several important contributions in the literature, such as combination of multiple surface EMG recordings to improve the SNR and the adaptive whitening filters to improve the statistical bandwidth, have not yet been used to improve torque estimations.

The experimental data used for the present research thesis are carried over from previous research. This prior research also modeled EMG amplitude to torque incorporating both agonist and antagonist muscles during tasks that involved force varying contraction. However, it avoided several of the earlier mentioned difficulties by examining constant posture efforts (similar to strict isometric conditions), whereas many of the above researchers examined fully dynamic tasks. These simplifications were intended to allow for an assessment of the newly developed EMG amplitude processors. The results were positive demonstrating a clear improvement in torque prediction when advanced processing techniques were used to obtain EMG amplitudes. This present research is anticipated to further investigate the results for more profound knowledge and to re-examine the encountered model convergence problems.

CHAPTER 3. SURFACE EMG TO TORQUE MODEL DESIGN

In the previous chapter there was a brief review of the literature achievements on EMG-torque relationship. As mentioned, there is not any generic model established yet, therefore researchers create models that best fit their design application or that are derived from earlier experimental work (Hill-type model). The primary focus of this research thesis was not to find the best model, but rather demonstrate the importance of incorporating the advances of EMG amplitude processing into each model. Hence, the results presented in later chapters will display the improvements in EMG-torque model performance as a function of EMG amplitude method. Since the EMG-tension relationship for each individual muscle is not possible, the EMG-torque relation can alleviate some issues such as measurements for mechanical verification, co-contraction, and cross-talk. This chapter describes the design process of a linear EMG-torque model that will be used to compare four different types of processors.

3.1. EMG-TORQUE MODEL DESIGN

This section is a summary of the theory involved to design the EMG-torque model. The concept of torque for the skeletal muscles is derived from the motion of the bones about a joint due to muscle contractions. Since surface EMG signal measures the activity of the skeletal muscles, a mathematical relationship can be established between the EMG amplitude and net joint torque. Using the principles of system identification, the model is standardized to a parametric type ARX (FIR) model.

3.1.1. Physical Interpretation of the EMG-Torque Model

The level of the tension produced in the muscle is controlled through the recruitment of motor units and their firing rate adjustments. The motor recruitment is hypothetically[1] done orderly based on the size of the muscle fibers. For tasks that involve slow force variations, as the tension level varies from low to high, the low frequency motor units are the first to be activated while the ones with high minimum frequency are the last [Hannerz, 1974]. The tension developed by the muscle also depends on both the conduction velocity and the geometry of the muscle fibers. The assumption that muscular force depends only on the firings of the motor units (rate and number of units) makes the relation between EMG to force non-linear in a sense that the number of MUs recruitment is higher for the higher contraction levels. As mentioned, the dependence on the conduction velocity and the geometry dependent parameters also contribute to the non-linearity.

The surface EMG is a non-invasive, easily obtained, measure of electrical activity in the skeletal muscle. Since both electrical and mechanical activities are mutually related through several mentioned physiological parameters, relating EMG amplitude to muscle tension would be ideal. However, there are two fundamental issues with this model. First, it is extremely difficult to measure EMG from only one muscle. In practice, surface mounted electrodes capture EMG generated from the muscles in a surrounding area, which are not necessarily the ones under investigation. This condition, known as cross-talk and already discussed in Section 2.1.3, is one of the main factors affecting EMG signal interpretation. Additionally, there is no practical method for

[1] Based on the EMG models created for isometric low force level contractions

accurately measuring the tension provided by an individual muscle. These two factors prevent the use of EMG amplitude to force models in terms of isolated muscle contribution as a method for evaluating performance of an EMG amplitude estimator [Clancy and Bouchard, 2001].

Another mechanical activity commonly related to EMG is the torque produced about a joint as muscular force is exerted. The problem of cross-talk is still present. Although unlike in the case of EMG to individual tension relation, it is not as influential to the net torque estimates [Clancy, Morin, and Merletti, 2002]. In addition, the model performance can be easily quantified by comparing the torque estimates to the actual torque about the joint that can be measured using a dynamometer. The prediction of the net torque requires the usage of both agonist and antagonist muscles. Muscles that perform a desired action are known as agonist muscles, whereas those that oppose the action are antagonist.

Some researchers have separated the contributions of agonist and antagonist muscles, assuming that the agonist muscles are inhibited while the antagonist ones are contracted. Doing so, the net torque is a result of the inhibition or agonist muscles [Lawrence and De Luca, 1983; Vredenbregt and Rau, 1973; Woods and Biggland-Ritchie, 1983; Zuniga and Simons, 1969]. On the other hand, Hasan and Enoka (1985) have experimentally determined the existence of co-contraction in contraction levels exceeding 20% MVC. Therefore, in the cases of 50% MVC it is necessary to acknowledge the contribution of both agonist and antagonist muscles.

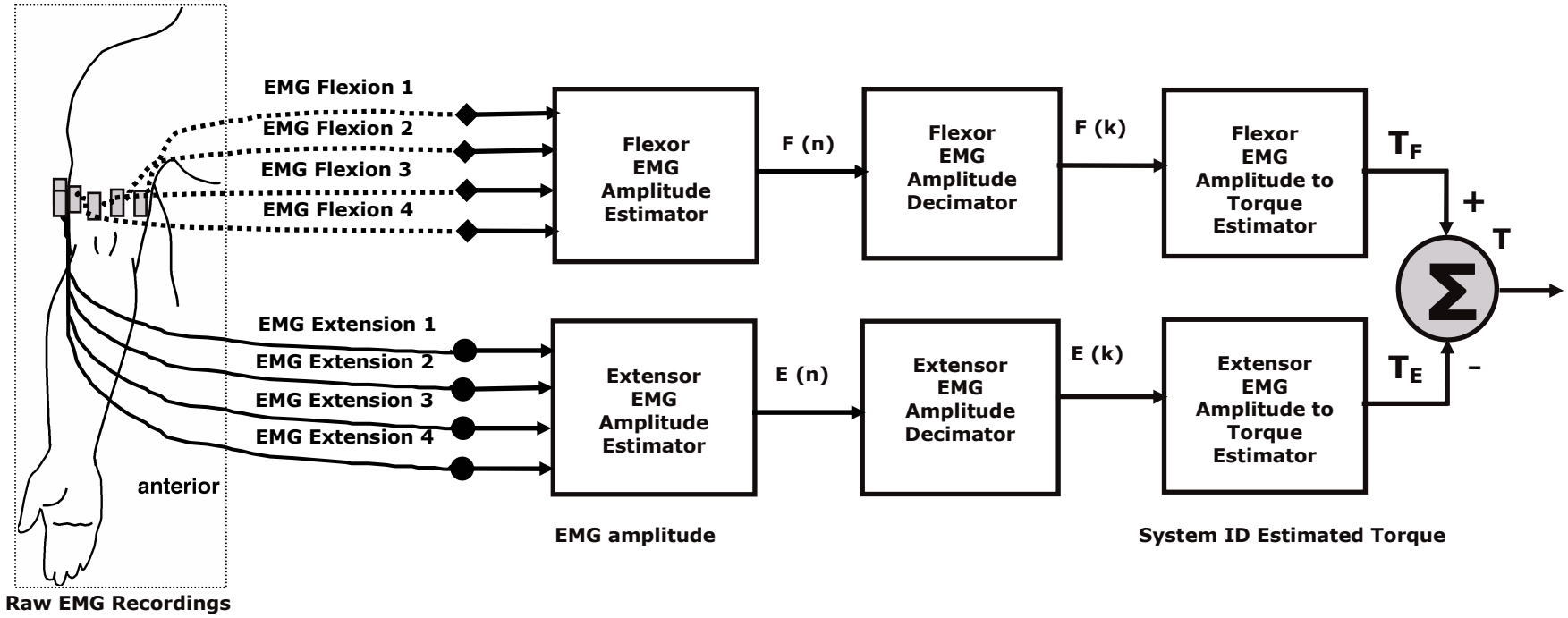

Figure 3.1: Raw Surface EMG to Torque Model [Clancy and Hogan, 1997]

Four surface electrodes affixed on top of the muscles (biceps and triceps) record the EMG signals. After amplified, filtered, and sampled they are applied to the EMG amplitude processor. The EMG amplitude estimations for flexion F(n) and extension E(n) are decimated to obtain F(k) and E(k) respectively. The amplitude estimates are used as two inputs to a system identification algorithm to predict the net torque about the joint (T).

Figure 3.1 shows a block diagram modified from the diagram from Clancy and Hogan (1997) and represents the model that is used to predict torque about the elbow joint from biceps and triceps muscle groups considering both agonist and antagonist muscles. Even though the contributions of flexion and extension are attributed to agonist and antagonist muscles, the model is designed based on their algebraic sum, rather than their independent contributions. The EMG amplitude processing (first stage from the left of Figure 3.1) and the data pre-processing (second stage in the same figure) stages will be discussed in detail in subsequent chapters. For now, it is assumed that the data are available and ready to be used in the EMG-torque model.

3.1.2. Mathematical Modeling for EMG-torque

Several studies, as mentioned in section 2.3.3, have determined that there exists a mathematical relationship between EMG-torque (linear or nonlinear). The internal change in the muscles may be produced by processing the EMG signal [Perry and Bekey, 1981]. It is not clear whether non-linear or linear models are the best choice. The linear models are widely used because of the simplicity in their design associated with the linear least squares solution [Inman et al, 1952; Thelen et al. 1994; Clancy et al., 2001], whereas the researchers using nonlinear models argue that they better describe the EMG physiological nature [Solmonow et. al, 1986; Vredenbregt and Rau, 1973; Woods and Biggland-Ritchie, 1983; Zuniga and Simons, 1969].

Without generalizing the model results, Gottlieb and Agarwal (1977) related EMG to torque using the following transfer function:

$$G(s) = \frac{F(s)}{E_{RA}(s)} = k \frac{1}{T_1 s + 1} \cdot \frac{1}{T_2 s + 1} \qquad (3.1)$$

where E_{RA} is the EMG amplitude obtained from the averaged rectifier output [Gottlieb and Agarwal, 1977]. This model is the Laplace transform of the differential equation with two degrees of freedom (time constants) and it assumes a continuous time domain system/signal, but it is agreed that it is easier to work with difference equations that represent the system for discrete time signals (samples). The conversion amongst them is straight-forward if the sampling rate is known. Another limitation is that the model can be used only for "isometric" tasks, because it does not include any physiological parameters (e.g. joint angle).

The model used for the purpose of this thesis is created by modifying the EMG-torque (ARX) model used by Stephan Bouchard (2001). The proposed model is an FIR (zeros-only) model and the degrees of freedom depend on the order of the system. Bouchard's model includes the feedback matrix of the ARX model, which is equivalent to the poles of a system. Even though it may require higher order to capture all the dynamics of a system, a zeros-only model is mathematically possible and easier to implement. The model form is written as:

$$\begin{aligned} T(k) = \quad & -e_1 E(k-1) - e_2 E(k-2) - \cdots - e_{nb} E(k-nb) \\ & + f_1 F(k-1) + f_2 F(k-2) + \cdots + f_{nb} F(k-nb) \end{aligned} \tag{3.2}$$

Referring to Figure 3.1 that shows the complete EMG-torque modeling process and the above equation, the decimated flexion [F(k), where k is the decimated discrete-time sample index] and extension [E(k)] EMG amplitudes were related to torque [T(k)] via the dynamic, linear, FIR model [Ljung, 1999, pp. 80–83]. In equation 3.2, the e_i represent the extensor model coefficients, the f_i are flexor model coefficients. The nb is the model order as defined in section 2.3.2. The model mathematical expression in 3.2 does not

change for the time-varying EMG amplitudes that are not decimated, therefore only the final results are presented.

3.2. MODEL SOLUTION

The model represented in equation 3.2, is the FIR version of the ARX model. This model is obtained using the standard linear difference equation of the ARX model that is found using the information given in Table 2.2 [Ljung, 1999]. Ljung writes the general model as:

$$y(t) + a_1 y(t-1) + \ldots + a_{na} y(t-na) = b_1 u(t-1) + \ldots + b_{nb} u(t-n_{nb}) + e(t). \quad (3.3)$$

The adjustable parameters in the equation are put in matrix form

$$\theta = [a_1\ a_2 \ldots a_{na} \quad b_1\ b_2 \ldots b_{nb}]^T. \quad (3.4)$$

The FIR model used for EMG-torque is the special case of ARX, obtained by setting the parameter $na=0$. The system is dual input – single output, therefore the equation is adapted for the MISO case. In equation 3.2, the coefficients $-e_1$-$_{nb}$ and f_1-$_{nb}$ represent Ljung's $b_{1\text{-}nb}$ coefficients. Analogous coefficient matrix is given by:

$$\theta = [-e_1 \ -e_2 \ldots -e_{nb} \quad f_1\ f_2 \ldots f_{nb}]^T \quad (3.5)$$

The vector of the known input EMG amplitude samples (decimated) are represented in the φ(k) vector. If the measurements are repeated over time then the vector φ(k) becomes a matrix with N rows, where N is the number of samples. In general N >> *nb* for the system identification to be possible. The inputs to this EMG-torque model φ(k) are written as:

$$\varphi(k) = \left[\begin{array}{lll:lll} E(k) & E(k-1)\ldots & \ldots.E(k-nb) & F(k) & F(k-1)\ldots & \ldots F(k-nb) \\ E(k+1) & E(k)\ldots & \ldots.E(k+1-nb) & F(k+1) & F(k)\ldots & \ldots F(k+1-nb) \\ \ldots. & \ldots. & \ldots & \ldots & \ldots & \ldots \\ E(k+N) & E(k+N-1)\ldots & ..E(k+N-nb) & F(k+N) & F(k+N-1)\ldots & \ldots F(k+N-nb) \end{array}\right]$$

The output matrix T(k) for N samples is given by:

$$T(k) = \begin{bmatrix} T(k) \\ T(k+1) \\ .... \\ T(k+N) \end{bmatrix} \qquad (3.6)$$

The problem involves solving the equation 3.7 to obtain the coefficient matrix.

$$T(k) = \varphi(k) \cdot \theta^T \qquad (3.7)$$

The solution can not be obtained by taking the inverse of the data matrix, $[\varphi(k)]^{-1}$, because the inverse of the matrix exists only for square matrices (in this case the number of the unknowns exceeds the number of the existing linear equations). Therefore there is not a unique solution, but rather a method referred to as linear squares error minimization of error can be used to obtain the "best-fit" coefficient matrix. The optimal value for θ is referred to as $\hat{\theta}$ and is given as:

$$\begin{aligned} \hat{\theta} &= \arg\min_{\theta}(\|T(k) - \varphi(k) \cdot \theta\|) \\ &= \arg\min_{\theta}[(T(k) - \varphi(k) \cdot \theta)^T (T(k) - \varphi(k) \cdot \theta)] \\ &= \arg\min_{\theta}[T(k)^T T(k) - T(k)^T \varphi(k)\theta - \theta^T \varphi(k)^T T(k) + \theta^T \varphi(k)^T \varphi(k)\theta] \end{aligned} \qquad (3.8)$$

Applying vector calculus concepts, the minimum is denoted as the value at which the gradient of the matrix is zero. Hence, the minimum value of $\hat{\theta}$ is found by computing the gradient of the difference between the measured output and the predicted output $||T(k)-\varphi(k)\theta||$. Therefore the coefficient matrix producing minimum error is equal to $\hat{\theta}$. The gradient of the error matrix is expressed as:

$$\Delta E(\theta) = -T(k)^T \varphi(k) - T(k)^T \varphi(k) + 2T(k)^T \varphi(k)\theta \qquad (3.9)$$

Equating the expression to zero, and solving for θ, yields to the minimization matrix in the least squared sense.

$$
\begin{aligned}
&-T(k)^T \varphi(k) - T(k)^T \varphi(k) + 2\varphi(k)^T \varphi(k) \cdot \hat{\theta} = 0 \\
&2\varphi(k)^T \varphi(k) \cdot \hat{\theta} = 2T(k)^T \varphi(k) \\
&\hat{\theta} = [T(k)^T \varphi(k)] \cdot [\varphi(k)^T \varphi(k)]^{-1}
\end{aligned}
\tag{3.10}
$$

After calculating $\hat{\theta}$, an estimate of the torque about a joint can be calculated as the product of the EMG amplitude estimates from both extensor and flexor muscles and $\hat{\theta}$. In practice, the coefficient matrix $\hat{\theta}$ is computed using a "training" dataset, then the resulting $\hat{\theta}$ is used to estimate the torque produced by another independent "test" dataset. The difference between the estimated torque and the real torque in the test dataset is the error and it is used to quantify the model performance. More on the testing procedure will be described in subsequent chapters.

CHAPTER 4. DATA COLLECTION AND ANALYSIS METHODS

This chapter explains the data collection method that followed some of the described literature suggestions. Then, it continues by describing the process of obtaining EMG amplitudes from four different processors. The EMG amplitude estimates are also decimated to improve the model performance by eliminating erroneous spikes existent in estimated torque as will be in detail discussed later. The entire pre-processing procedure is presented in a block diagram form and it is utilized as necessary during performance testing. System identification involves two main steps, training and validation. During training, a coefficient vector is fit to the input data based on the least squares error minimization. Model validation requires utilizing a distinct dataset to estimate the output using the optimal coefficients. The train-test along with model performance measures procedure is explained in detail in the present chapter.

4.1. EMG DATA COLLECTION

Recording the EMG signal using surface electrodes faces challenges related to the signal power and external/internal noise. As explained earlier, some of the internally generated noise found in EMG system can neither be eliminated nor reduced. However, errors due to recording devices, electrode placement, skin effects, and some other external error sources (2.1.3) can be reduced by taking the necessary precautions. This data collection section explains some of the potential noise sources along with some suggestions for minimization and then it continues by describing the experiment conducted to collect the EMG data used in this project. The description of the apparatus and experimental procedure is brief, since the experiment is not part of this thesis

contribution. More details can be found elsewhere [Clancy, 1999; Bouchard, 2001; Clancy and Farry, 2000].

4.1.1. Noise Reduction Precautions

One of the most important sources of error in EMG recording is the placement of the electrodes. The tight spacing of the electrodes in a multiple channel recording can produce correlated signals, increases the chance of short circuits, and enables electrical coupling. In addition, the PSD of the recorded EMG signal depends on the location of the electrode in relation to the innervation zone (MUAP generation site) the myotendon zone and the lateral edge of the muscle [De Luca, 2002]. The center position between the innervation on the top and myotendons on the bottom is preferred (see Figure 4.1).

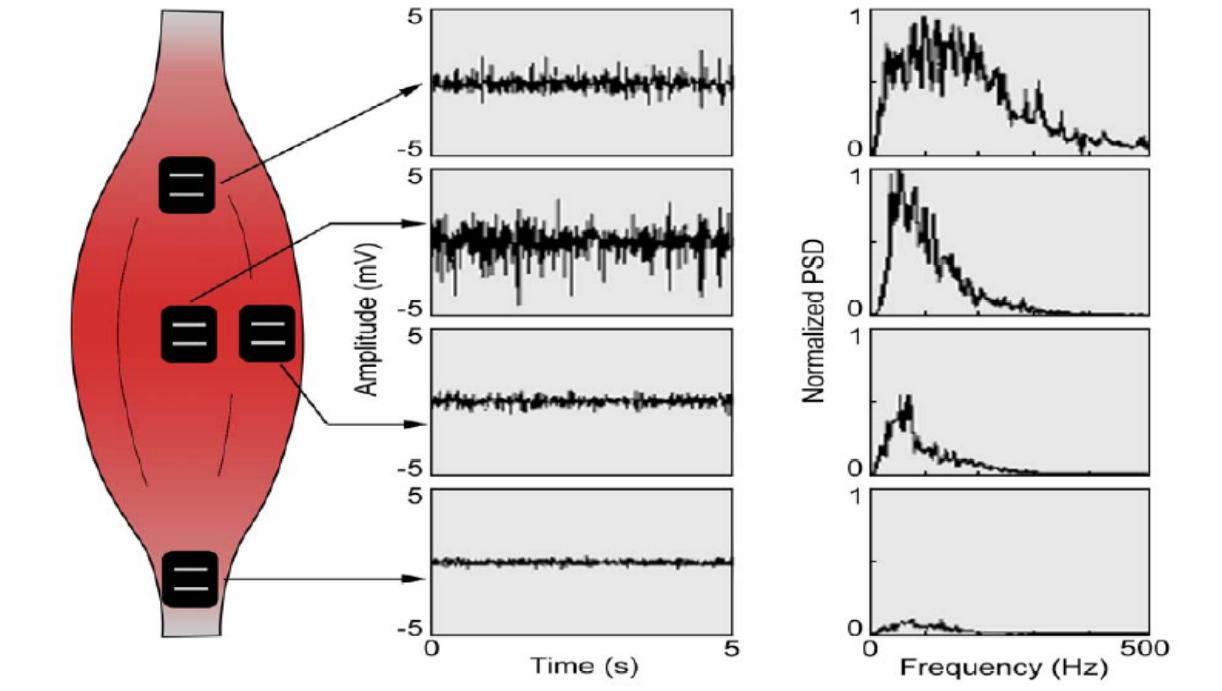

Figure 4.1: EMG Electrode Placement [De Luca, 2002]

The principle of EMG electrode functionality derives from a layer of charge created in the interface between the metal of the electrode and an electrolyte solution. The charge layer creates a potential gradient that translates into voltage picked up by the electrode. The voltage is dependent on the type of the electrode material, hence it is crucial to use electrodes of the same material to minimize the potential difference (especially in a multi-channel application). In addition, some of the power of the initial EMG signal is lost due to the effect of skin-electrode impedance. To reduce its impedance, skin is prepared using conducting-paste, rubbing alcohol, or lipid solvents. The amplifier is also chosen to have input impedance at least 100 times more than expected electrode-skin impedance, thus reducing the power loss even more. [Clancy, Morin, and Merletti 2002]

Surface electrodes suffer from motion artifact due to displacement and deformation (stretch) of the underlying skin. Both effects are minimized by cleansing the skin with solvents, rubbing a conductive paste, and affixing the electrodes carefully prior to recording EMG. Motion artifacts can also be reduced through signal conditioning both on-line and off-line. Since the typical power density of these types of motion artifacts is below 20 Hz, they can be largely attenuated using high-pass filter at that frequency either in the processing software or integrated in the hardware [Clancy, Morin, and Merletti 2002].

The cables of the electrodes have an intrinsic capacitance, which if exposed to a varying magnetic field (electric field) can produce alternating currents (1-50Hz). The cumulative effect of the voltage created by the product of the skin-electrode interface impedance and the displacement current in addition to the magnetic coupling in some

cases is comparable to the magnitude of the real EMG. Shielding the cables can improve the magnetic environment, although electrostatic discharges spreading through measurements can be a harmful side effect [Clancy, Morin, and Merletti 2002]. The usage of active electrodes is a better solution, because the voltage buffer transforms high impedance at the electrode to low impedance at the output where the signal is fed to the cables [De Luca, 2002].

The interference of power line current and its harmonics (60 Hz in U.S. and 50 Hz in Europe) can have power densities larger than EMG itself and are a commonly appearance in EMG recordings. The effect of the power lines can be reduced by notch filters at 60Hz or by differential amplifiers that have a high common mode rejection ratio (CMRR). The second is preferred, because the notch filters omit real signal in addition to the noise. A CMRR of 90 dB is generally advised in the literature, even though current technology can provide a CMRR of 120dB. The reasons for not using amplifiers with 120dB at CMRR are the price, their stability, and the power line signal may not be in phase [De Luca, 2002].

4.1.2. Apparatus and Experimental Procedure [ii]

The experiment conducted to collect this set of EMG data was consistent with the suggestions mentioned in the previous section (4.1.1) and literature [De Luca, 2002; Merletti, 1999; Clancy, Morin and Merletti, 2002] for noise minimization. The data collection experiment was conducted previously; thus, the experiment description is summarized from other sources [Clancy, 1999; Bouchard, 2001; Clancy and Farry, 2000]. The subjects had signed consent for their participation and proper human studies

[ii] Parts of this section are taken from the paper submitted to the Journal of Biomechanics (attached to Appendices) authored by Clancy, E.A; Bida, O.; Rancourt, D.

permission was taken prior to the experiment. The apparatus (Figure 4.2) used to collect the EMG data was a Biodex exercise machine (Biodex Medical Systems, Inc., Shirley, NY). Each of the subjects were seated in a lightly cushioned seat and secured using seatbelts. The subject's right arm was positioned in the plane parallel to the floor, with the shoulder abducted 90^{o}, the forearm oriented in the parasaggital plane, the wrist fully supinated and the elbow flexed 90^{o} (Figure 4.4). The wrist was rigidly attached to the Biodex dynamometer with a cuff at the styloid process. The position of the dynamometer was maintained throughout the entire experiment [Clancy, 1999].

Figure 4.2: Biodex Exercise Machine for the Experiment [Bouchard, 2001]

The skin above the investigated muscles was cleaned with an alcohol wipe and a small amount of conducting paste was used to rub the subject's arm. The EMG active amplifying electrodes (Liberating Technologies Inc. model MYO115, Holliston, MA) were placed over each of the biceps and triceps muscles, midway between the elbow and the midpoint of the upper arm, centered on the muscle midline. The two contacts (4 mm diameter, stainless steel, separated 15 mm center-to-center) of each electrode-amplifier (Figure 4.3) were oriented along the muscle's long axis. Adjacent electrode-amplifier centers were spaced 1.75 cm apart, transversely across the arm. The ground electrode was applied over the acromion process. Each electrode-amplifier had a gain of 725, a common mode rejection ratio of 90 dB at 60 Hz, and a second-order 10–2000 Hz bandpass filter.

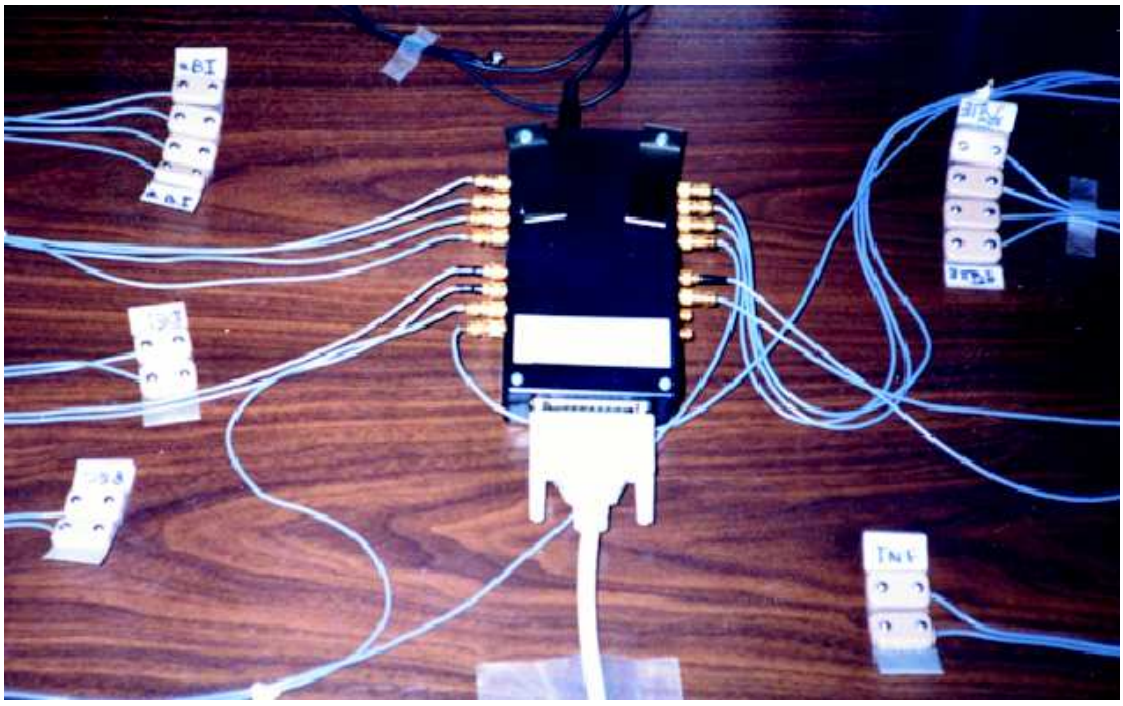

Figure 4.3: Surface EMG Electrodes and Acquisition Box [Bouchard, 2001]

The output from each of the electrode-amplifier was electrically isolated, amplified, and low pass filtered (fourth-order filter at 2000 Hz). Amplification stage

contained a negative gain configuration standard opamp with a selectable gain (-1 to -25). Recordings with the two contacts of each electrode-amplifier shorted gave a measure of equipment noise, which averaged 2.1±1.7% of the root mean square EMG at 50% maximum voluntary contraction (MVC). The EMG and dynamometer signals were sampled at 4096 Hz using a 16-bit A/D converter (Computer Boards model CIO-DAS1600/16, Mansfield, MA).

Fifteen healthy subjects (eight male, seven female; aged 23–65 years) each completed one experiment.

Table 4.1: Subject Information (Code, Age, and Gender)

SUBJECT CODE (Exp. LB)	AGE	GENDER
02	31	F
03	49	M
05	29	F
07	65	M
08	43	F
09	60	M
10	41	F
12	62	F
13	50	M
16	28	M
17	58	F
18	41	M
19	31	F
20	23	M
21	65	M

Subjects initially performed two 2 second MVCs each in flexion and extension, the averages of which were used as the subject's MVCs for the experiment. Next, they performed a 0% MVC (rest contraction) and separate flexion and extension 50% MVCs for five seconds, utilizing force feedback on a computer screen. These contractions were used to calibrate the advanced EMG amplitude processors [Clancy and Farry, 2000].

The subjects then performed dynamic (constant-posture, force-varying) target tracking contractions positioned as in Figure 4.4. A computer screen displayed either their elbow joint torque (the dynamometer signal) or the algebraic difference between real-time biceps and triceps EMG amplitude, as a biofeedback signal. The EMG amplitude difference provided a biofeedback signal that was similar in character to the torque feedback, albeit with increased variance. The computer produced a second "pursuit" display on the screen which moved randomly between 50% MVC extension and 50% MVC flexion. The random pursuit profile followed a uniform random distribution with a bandwidth of either 0.25 Hz (slow tracking) or 1 Hz (fast tracking).

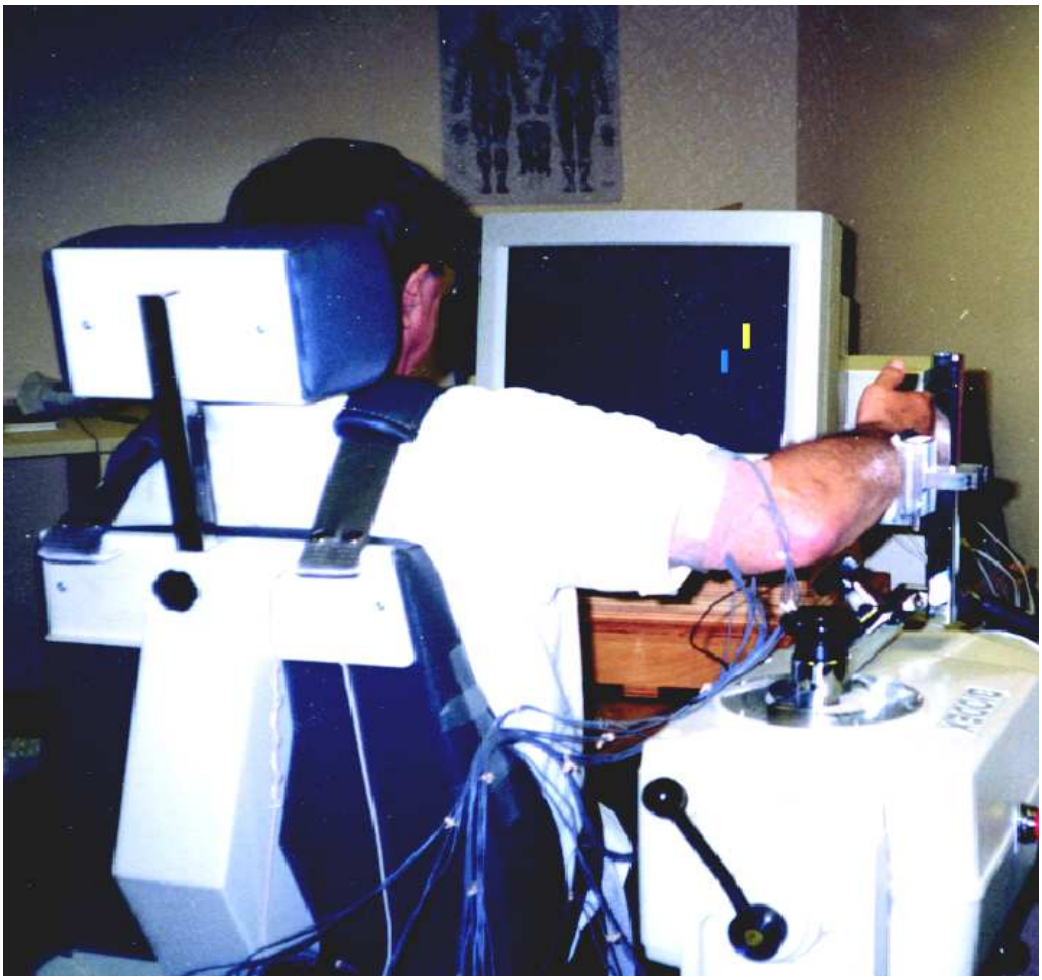

Figure 4.4: Subject During Experiment [Bouchard, 2001]

Subjects completed 15 slow tracking trials (three sets of five) and 15 fast tracking trials (three sets of five), each of 30 s duration. The subject's arm was removed from the wrist cuff between all recording trials to allow 2–3 minutes of rest to avoid fatigue.

4.2. EMG AMPLITUDE ESTIMATION METHOD

For the present study, all data analysis was performed off-line using MatLab (The Mathworks, Natick, MA). In order to determine the influence of amplitude processors on torque estimation, four different EMG amplitude (EMGamp) processors were compared. In each case, an amplitude estimate was produced in six stages separately for the biceps and triceps muscle groups (Figure 2.5). The design of the EMG amplitude processor is explained in detail in the background chapter, while this section describes the experiment in a more practical perspective. Before creating amplitude estimates from the raw EMG data (stored in forms of A/D channels for each of the electrode locations), it was necessary to calibrate the noise-rejection, adaptive whitening, and spatial uncorrelation. The calibration requires the additive noise signal, which in this case is the 0% MVC signal recorded while subjects were fully resting. This recording is assumed to capture the 60 Hz noise as well. The electrode locations encoded in the channel number are given in Table 4.2 and further description is found in the APPENDICES: (I). The A/D channels 1-4 are used to estimate biceps EMG amplitude and channels 8-11 are used to estimate triceps EMG amplitude in multiple channel processing. In the case of single channel processing, channels 2 and 9 are used for flexion and extension EMG amplitudes, respectively.

Table 4.2: A/D Electrode Channels from the Experimental Data

A/D Channel	Contents
1	EMG: Biceps, most lateral location
2	EMG: Biceps, lateral center
3	EMG: Biceps, medial center
4	EMG: Biceps, most medial location
8	EMG: Triceps, most medial location
9	EMG: Triceps, medial center
10	EMG: Triceps, lateral center
11	EMG: Triceps, most lateral
16	Dynamometer

For all processors (Table 4.3), the EMG data were first high-pass filtered at 15 Hz using a non-causal, effective 10^{th} order, FIR filter. The detection was performed with an absolute value operation (MAV, d=1) and the smoothing stage was omitted, since smoothing was incorporated within the subsequent pre-processing step.

Table 4.3: Four Processors Types (Processor 1-4)

Single Channel Unwhitened (S-CH-UNWHIT)
Single Channel Whitened (S-CH-WHIT)
Multiple Channel Unwhitened (M-CH-UNWHIT)
Multiple Channel Whitened (M-CH-WHIT)

Processor type 1 is the single-channel, unwhitened processor. The raw EMG signal for each muscle group from one of the electrodes located centrally on the muscle was digitally high-pass filtered and rectified. Processor 2 is a single-channel, whitened processor obtained by adaptively whitening the same electrode channel as Processor 1 before the rectification stage. The adaptive whitening technique is explained briefly in section 2.2.4 and it has been implemented in a stand-alone MATLAB toolbox [Clancy, 2004]. Processor 3 is a four-channel, unwhitened processor. After rectification, the four EMG signals from a muscle group were normalized in magnitude and ensemble

averaged. Processor 4 is a four-channel, whitened processor. Each of the four channels from Processor 3 was adaptively whitened prior to rectification. The settings for optional properties for the amplitude estimation function can be found in APPENDICES: (II).

4.3. SYSTEM IDENTIFICATION PROCEDURE

After estimating the amplitudes off-line using the EMG toolbox, the data were further processed as necessary to improve the model performance [Ljung, 1999 pp. 386]. The torque estimates were then obtained using a train and test procedure, where the coefficients were computed using a train dataset and were validated using another dataset referred to as the test dataset. The performance of the model design was evaluated using conventional measures that will be discussed in detail in this section.

4.3.1. Data Pre-Processing

Some of the data manipulation to achieve the desired results involves normalization to % MVC and A/D offset subtraction for torque as well as decimation and truncation of both EMGamp(s), and torque (Figure 4.5). Normalization to maximal voluntary contraction % MVC is a common practice when trying to relate EMG to torque [Merletti, 1999]. The EMG amplitudes estimates were to % MVE (where 100% MVE - EMG amplitude level corresponding to 100% MVC) in extension/flexion units; hence, it was only necessary to normalize torque to %MVC according to either flexion or extension.

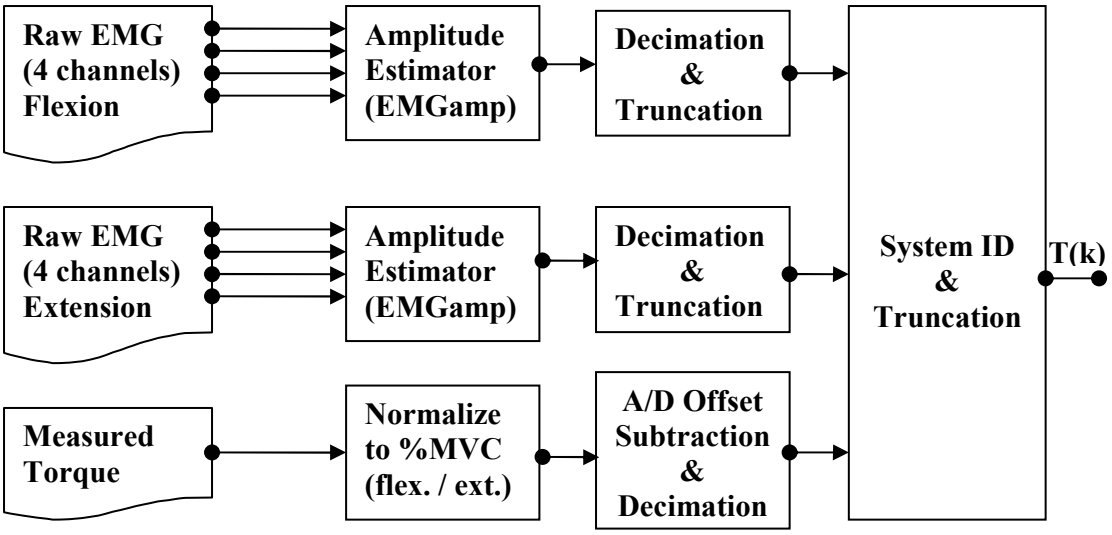

Figure 4.5: Block Diagram of EMG Data Pre-processing for System ID Algorithm

The next step common to both torque and EMG amplitudes (EMGamps) in Figure 4.5 is decimation. Because the raw EMG data were sampled at 4096 Hz, the EMG amplitude estimates were also produced at 4096 Hz. The flexion (biceps) and extension (triceps) EMGamps are the inputs to a system identification model in which elbow joint torque is the output. The torque output, however, has signal power over a *much* lower band of frequencies than raw EMG. Thus, the high sampling rate is unnecessary. Therefore, the EMGamps are decimated. The decimation rate was found by evaluating various integer-valued decimation rates from 1–900. In each case, the data were also low pass filtered with a cut-off frequency equal to half the new sampling rate (8^{th}-order Butterworth filter applied in the forward, then the backward time directions to achieve zero-phase) prior to down-sampling.

The data truncation was used to eliminate the transient effect of the filters on the signals (a.ka. a "startup" transient). The effect is seen as corruption only at the beginning if causal filters are used and in the case of non-causal filters both at the beginning and at

the end. Adding up the effect based on the orders of filters in each of the amplitude processing stages, it is necessary to subtract 500 ms on each side prior to system identification (ID) and 500 ms after it. The number of samples subtracted was based on the new decimated sampling rate. Additionally, A/D converter offset was subtracted from the torque signal to account for imbalance in the dynamometer output.

4.3.2. Torque Estimation Procedure

The EMG data used for this project were previously collected as described. Data were collected from fifteen subjects using a multiple channel data acquisition system. In addition to four channels of EMG amplitudes for each of the muscle groups, the torque about the elbow joint was measured using a dynamometer. As mentioned, for each subject, three sets of data recordings were performed. Within each set of three, data were recorded five times using various feedback mechanisms for controlling elbow torque. Each of these five subsets was recorded at two different tracking speeds (0.25 Hz and 1 Hz) totaling to $3 \times 5 \times 2 = 30$ sets of EMG data for each subject.

Referring to the model solution in section 3.2, it is required to fit a set of coefficients to the input data matrix (EMGamps for flexion and extension) to estimate torque. For convenience the model mathematical expression is repeated here:

$$\begin{aligned} T(k) = \quad & -e_1 E(k-1) - e_2 E(k-2) - \cdots - e_{nb} E(k-nb) \\ & + f_1 F(k-1) + f_2 F(k-2) + \cdots + f_{nb} F(k-nb) \end{aligned} \tag{4.1}$$

The optimal fit coefficients were determined using a linear least squares solution. The input data matrix φ(k) in section 3.2 was created using the toeplitz routine to increment the samples of amplitude estimation (flexion and extension) and the model order as in equation 4.1. The system solution involves matrix inversions that can be implemented

using QR-factorization (qr) or the pseudo-inverse (pinv). QR-factorization expresses the matrix as the product of a real orthonormal or complex unitary matrix and an upper triangular matrix. Pseudo-Inverse is the process of inverting an overdetermined linear system (matrix has more rows than columns). The advantage of using the QR-factorization method is computation simplicity due to elimination of redundancy [Kolman and Hill, 2001].

Since the results and the computation time for both methods were the same, only the results from pseudo-inverse techniques will be discussed. The model coefficients are determined utilizing a train-test evaluation routine. Specifically, coefficients were fit to the input data from a training trial and then used to compute the torque via equation 4.1 from a different test trial. The error signal is defined as the difference between the measured and the model estimated torques. If all possible combinations are used for the data combination, there would be a total of 30 × 29 combinations of training and test data sets. Because of the large computation time, a comprehensive cross-validation is sufficient for the scope of this research. Therefore, the 15 trials at a given tracking speed were organized as three sets of five contractions. (The two speeds are evaluated separately) Within a set, optimal coefficients were trained to one trial, and then tested on the four remaining trials. There were a total of 180 error signals available per type of processor (15 subjects × 3 sets per subject × 1 training trial per set × 4 test trials per training trial). As mentioned, one second of data from the beginning and end of each error signal was removed (trimmed), since these data were corrupted by the startup transients of the various processing filters.

In summary, the following parameters were varied in the computations performed using MatLab (R13, Version 6.5):

- EMG amplitude estimator type: single-channel-unwhitened, single-channel-whitened, multiple-channel-unwhitened, multiple-channel-whitened
- Integer-valued decimation rate subjectively chosen from 1 to 900
- Matrix inversion method either pinv. or qr factorization
- EMG-torque model order from 1 to 60

The performance of the model implemented for this research matches the performance obtained using the built-in ARX parametric model function in MatLab *System ID* toolbox. The toolbox is suggested to be utilized in the future, when more complicated models are necessary.

4.3.3. Model Performance Measures

The resulting EMG-torque error signal from 180 combinations for each processor type was investigated in several ways. The error mathematical expression used is:

$$Error(k) = \sum_{k=1}^{N} \left(\hat{T}(k) - T(k) \right) \qquad (4.2)$$

where N is the sample duration of the truncated estimated torque $\hat{T}(k)$ *and measured torque T(k)*. The measured torque was truncated to equate the number of samples with the estimated torque. All errors were normalized to twice the torque at 50% flexion MVC, denoted $\%MVC_F$. Throughout this thesis results of model performance will be evaluated using two main time domain error measures: the percent mean absolute error (%MAE) as computed for each trial

$$\%MAE = 100 \cdot mean\left(\left| Error(k) \right| \right), \qquad (4.3)$$

and the percent variance accounted for (%VAF), defined by Kearney [Kirsch, Kearney, Crago, 1994] as:

$$\%VAF = 100 \cdot \left(1 - \frac{\sum_{k=1}^{N} [Error(k)]^2}{\sum_{k=1}^{N} T^2(k)} \right) \qquad (4.4)$$

The power spectral density (PSD) of each error sequence was another method used to evaluate the error frequency distribution and identify the character of the error. The PSD was estimated using Welch periodograms (Hamming window, 1024-point FFT, 50% overlap).

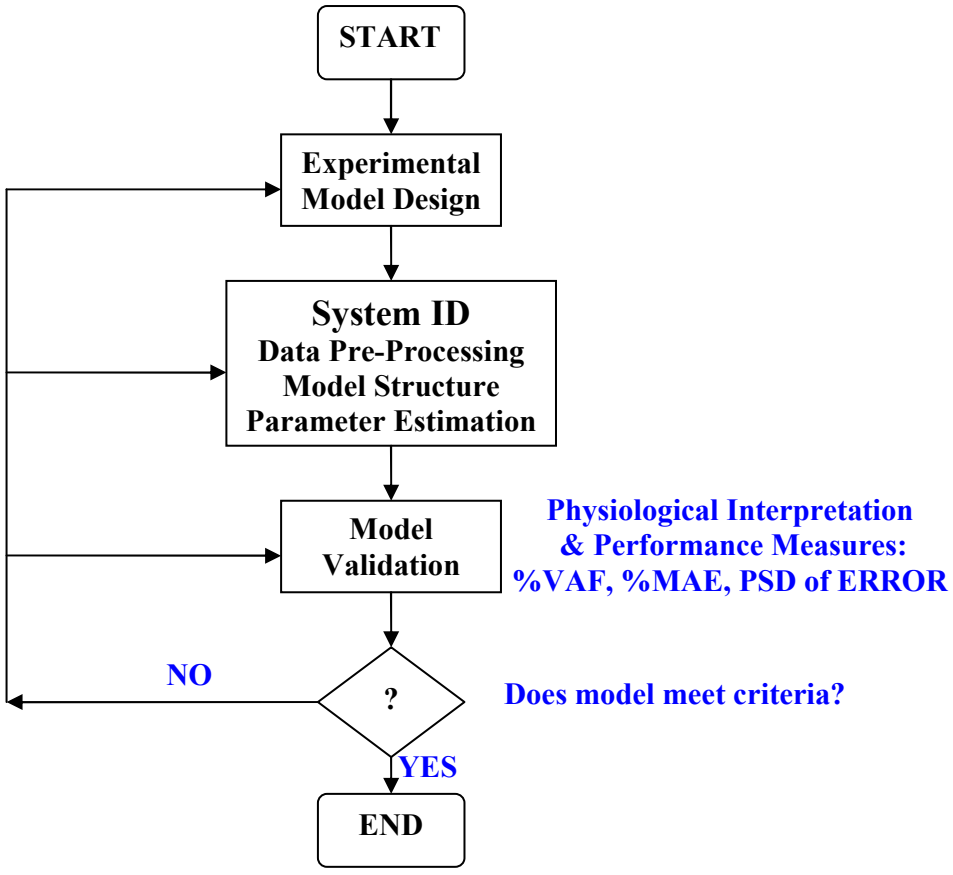

Figure 4.6: System Identification Procedure [Created based on Ljung, 1999]

The final stage of the system identification (System ID) procedure is the model validation. During this stage, the model performance results (%VAF and %MAE) are interpreted in the physiological sense of the real system behavior. If the expectations are not satisfied, then there is need for model re-design (Figure 4.6).

CHAPTER 5. PROJECT RESULTS

There were several important results derived after completing the described test procedure. This chapter starts with the decision on the final decimation rate as a solution to model non-convergence problems that were observed during prior research. Then, it continues with a graphical description of the model performance where the outcomes are contrasted for the four types of processors.

5.1. DECIMATION

The process of decimation includes low-pass filtering and down-sampling. Decimation is used if the system is over-sampled and if it contains high frequency noise components. The necessity for decimation prior to system identification was determined because some of the prediction torque sequences exhibited a few large "spikes." The observed errors were referred to as spikes because they had *much larger* amplitude compared to the test torque and lasted only a few samples (see Figure 5.1). The spikes occurred infrequently (~15% to 20% of combinations) but their magnitude caused the overall %VAF (and MAE) to be unrealistic. During prior EMG-torque work, the trials exhibiting the described error were considered to be "non-convergent" [Clancy *et al.*, 2001]. Figure 5.1 shows a typical example of observed torque spikes. The time domain torque plots are on the left of the picture. The amplitude of torques spiked to 20, 000 % MVC_F when there was no decimation (c.f., time sample about 2*10^4 when d=1).

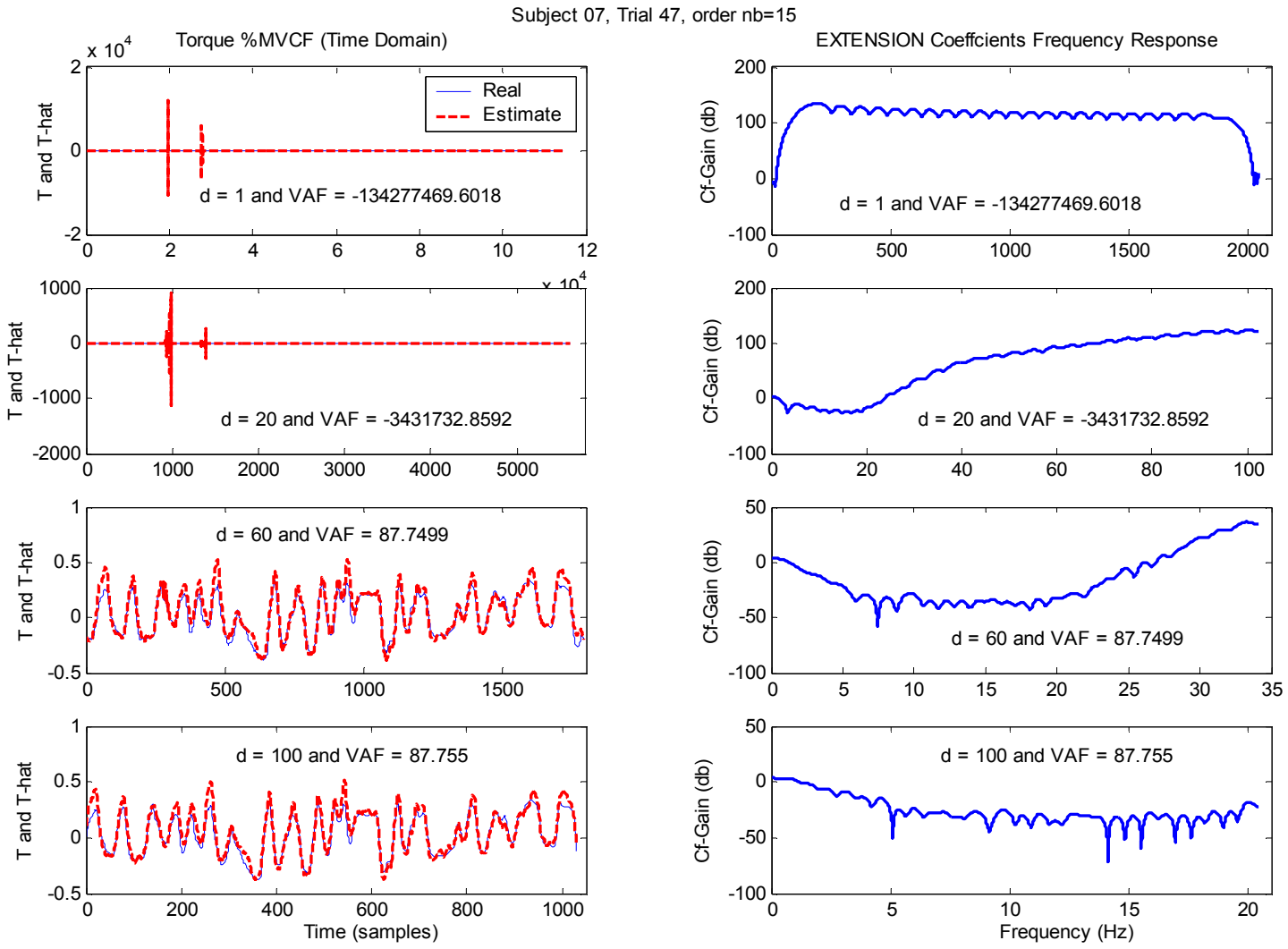

Figure 5.1: Changes of Predicted Torque while Increasing Decimation Rate

The figure above shows the transformations of the torque predictions as a function of the sampling rate. On the left side of the figure, the torques both predicted (red dashed line) and measured (blue solid line) are plotted versus sample time for four decimation rates (top to bottom: 1, 20, 60, and 100). On the right side of the figure, the gains of the coefficients computed during the system identification (extension) are plotted for each of the decimation rates. The purpose of this figure is the graphical presentation of the observed spikes. When the decimation rate is d=1 the torque amplitude exceeds 10^4 and the coefficients gain exceed 100 dB outside the system band (~ 4-10 Hz). As the

sampling rate is increased to d = 100 the model performance improves (%VAF = 87.755), the spikes disappear, and the left side gain plot shows the expected LPF like performance with a max gain of 0 dB. During previous research, where the spikes were initially observed, a decimation rate of 20 was utilized, but as seen in this figure that rate was not enough.

Further investigation demonstrated that the errors were related to sampling rate. The raw EMG sampling rate of 4096 Hz was more 1000 times the natural bandwidth of the EMG-torque system that contained 99.9% of the power within about 4 Hz, even at fast tracking bandwidth. Figure 5.2 shows the average torque power accumulation rate for fast tracking bandwidth.

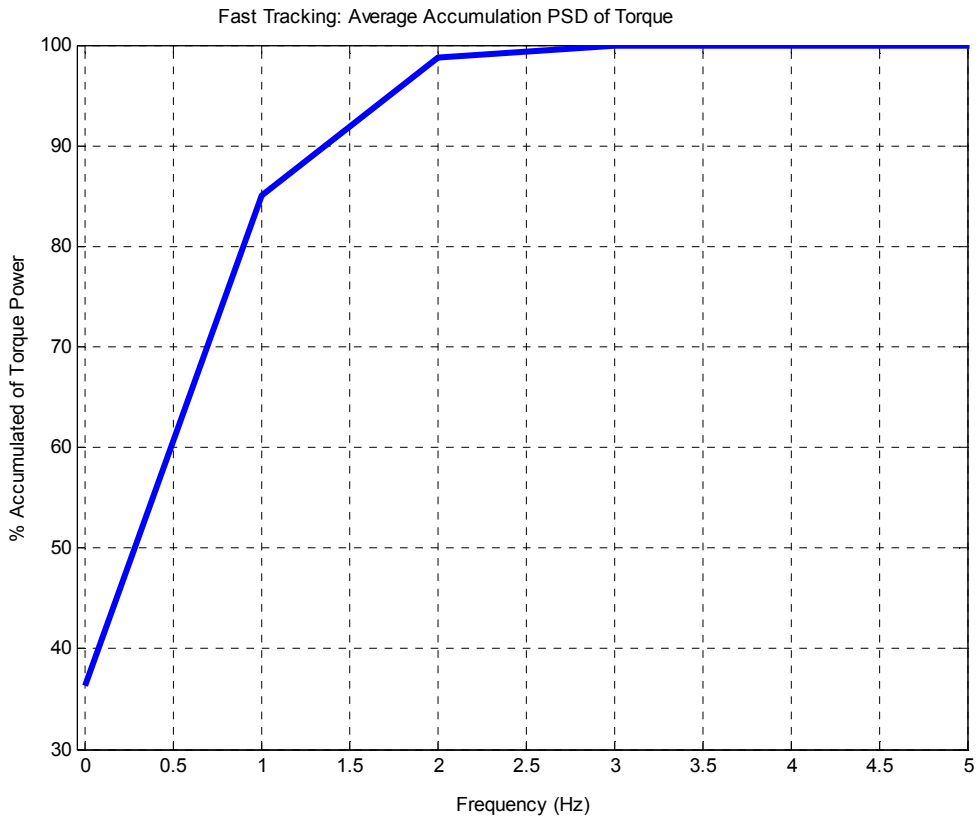

Figure 5.2: Signal Power Accumulation (average PSD torque) vs. Frequency

The occurrence of the noise spikes was associated with the cases that the system was calibrated with torque trials (training sessions to determine fit coefficients) that contained no power beyond 4 Hz (99% chance). If the test trials were contaminated with noise extended to larger frequencies, the system produces models with unrealistically high gain at frequencies above 4 Hz. The high gains beyond the system band are shown for a typical example on the right side of the picture (Figure 5.1). Hence, even a small amount of noise power at frequencies above 4 Hz in a test trial caused a noise spike in the predicted torque. Although the occurrence was infrequent because most of the torque power was contained within 4 Hz, they were an obstacle to further improvements. This phenomena encountered with oversampling is also described as common in the system identification literature [Ljung, 1999].

The solution to this problem was to decimate the EMG amplitude signals prior to performing the system identification. Progressively lowering the effective sampling rate, the spikes reduced both in occurrence rate and magnitude. A factor of decimation of 100 (effective sampling rate of 40.96 Hz) extinguished all observed spikes. As seen from the %VAF values plot in Figure 5.3 the performance of the EMG-torque saturates for rates above 100 and eventually decreases as the decimation rate exceeds 400. This eventual drop in the performance is due to the decrease of the cutoff frequency of the low-pass filter included in the decimation process. The low cutoff frequencies eventually remove signal power within the natural bandwidth. The optimal sampling rate of 40.96 Hz is approximately 10 times the highest signal frequency, which is consistent with the rate recommended by Ljung (1999) and captured all of the signal power. Concluding, the decimation rate of 100 is used to obtain the consequent results.

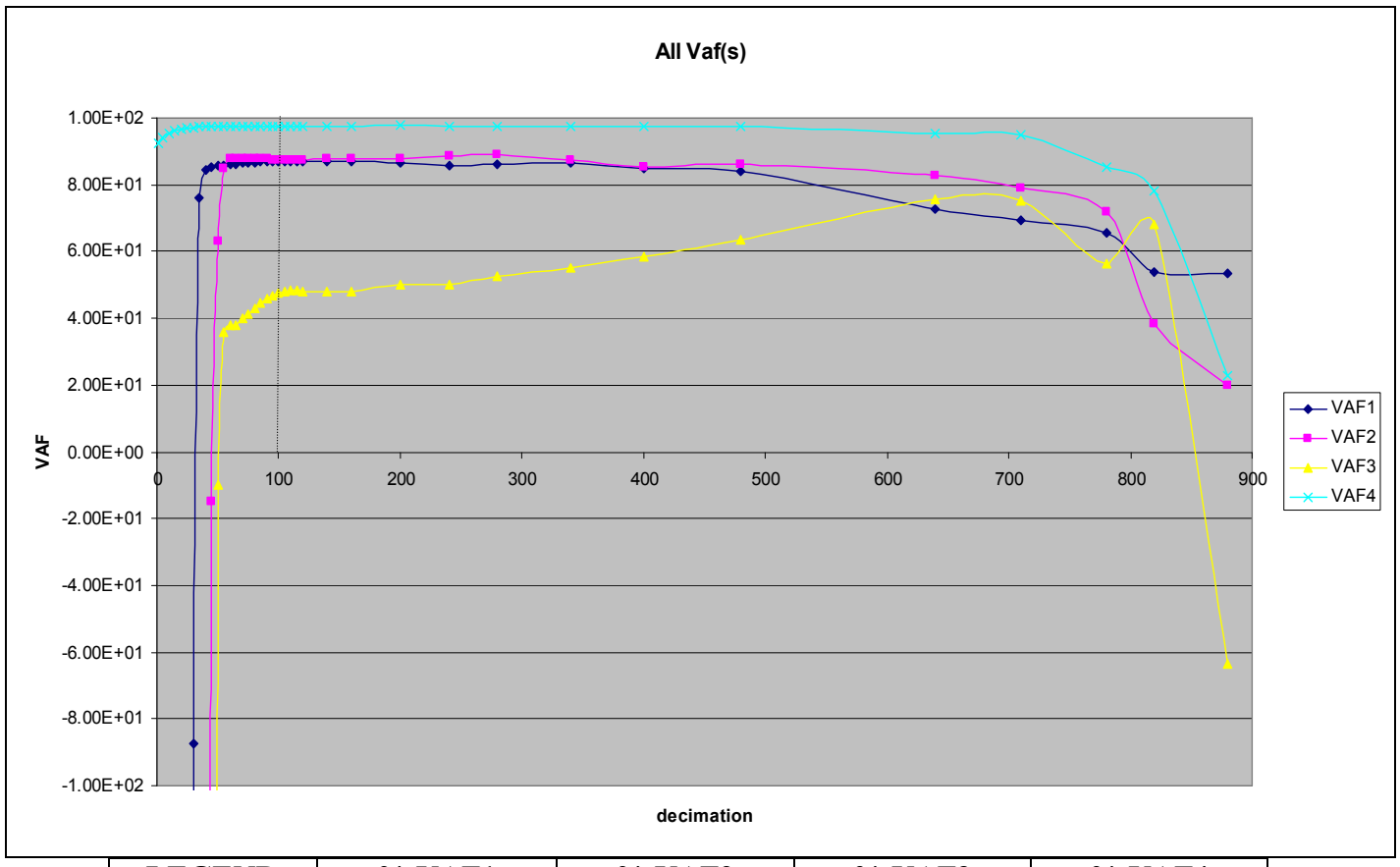

LEGEND	% VAF1	% VAF2	% VAF3	% VAF4
Subject:	02	07	20	04
Train Trial:	25	45	65	60
Test Trial	28	47	69	61

Figure 5.3: Decimation Rate Evaluation Plot

5.2. COMPARISON OF EMG AMPLITUDE PROCESSORS

Applying decimation with a factor of 100 and the additional pre-processing steps (truncation and A/D offset subtraction) described, the EMG amplitudes obtained from four different processors were used to estimate torque. The method of estimation is explained earlier hence this section presents the drawn results.

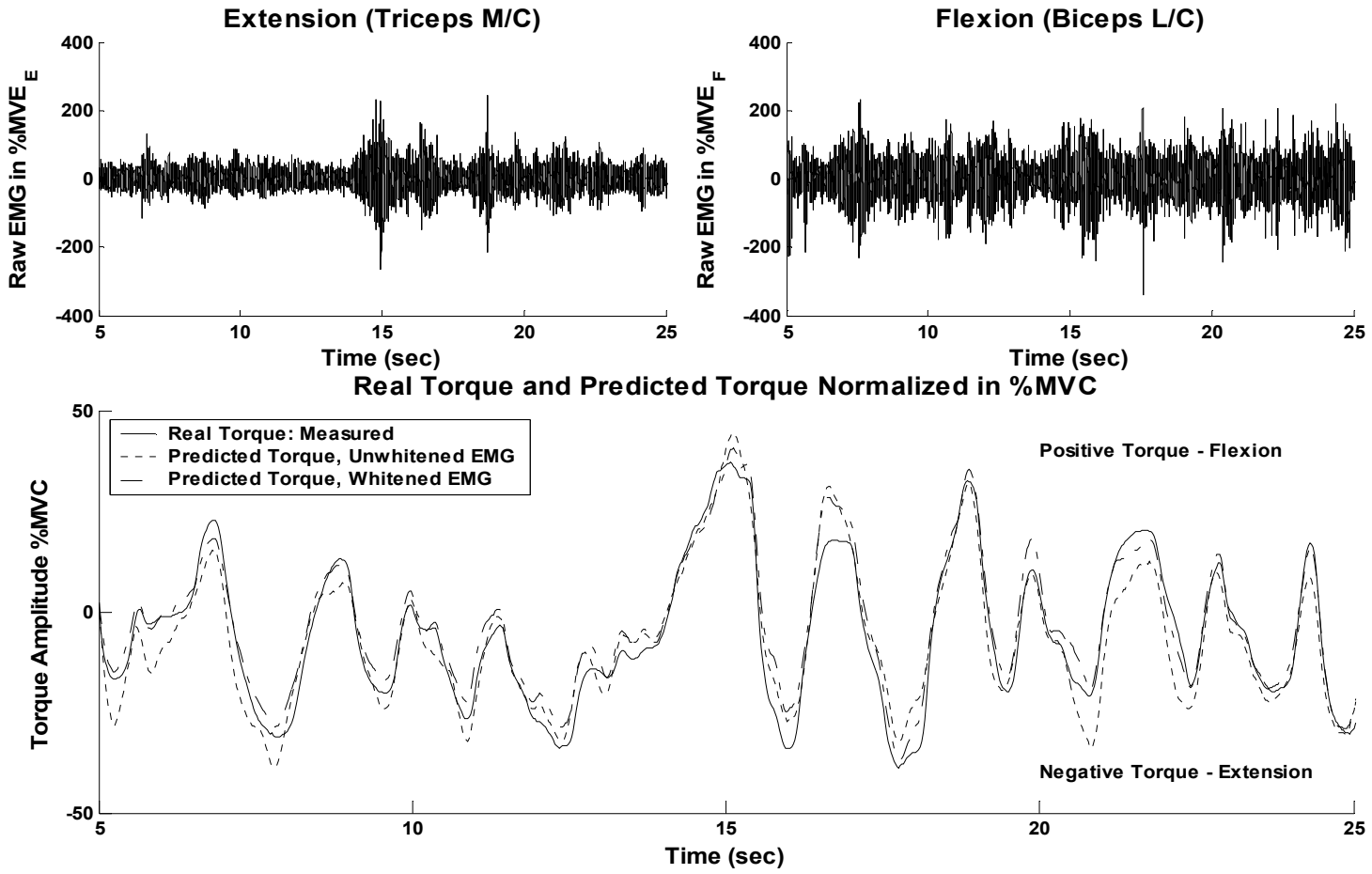

Figure 5.4: Raw EMG (flexion & extension) and Torques

Figure 5.4 shows the raw EMG signal and the predicted torque from two different processors in a typical example. The predicted torque in both cases captures most of the dynamics exhibited in the actual torque.

The values obtained for performance evaluating expressions, % MAE in eq. 4.3 and % VAF in eq. 4.4, were averaged across the 180 combinations for each processor. Figure 5.5 shows mean and median values of %VAF and MEA, as a function of the system identification model order, for each of the four EMG amplitude processors. The plot shows the results obtained for the fast tracking speed using PINV to invert matrices, whereas the slow tracking speed and the use QR-factorization performance results are shown in APPENDICES: (III)

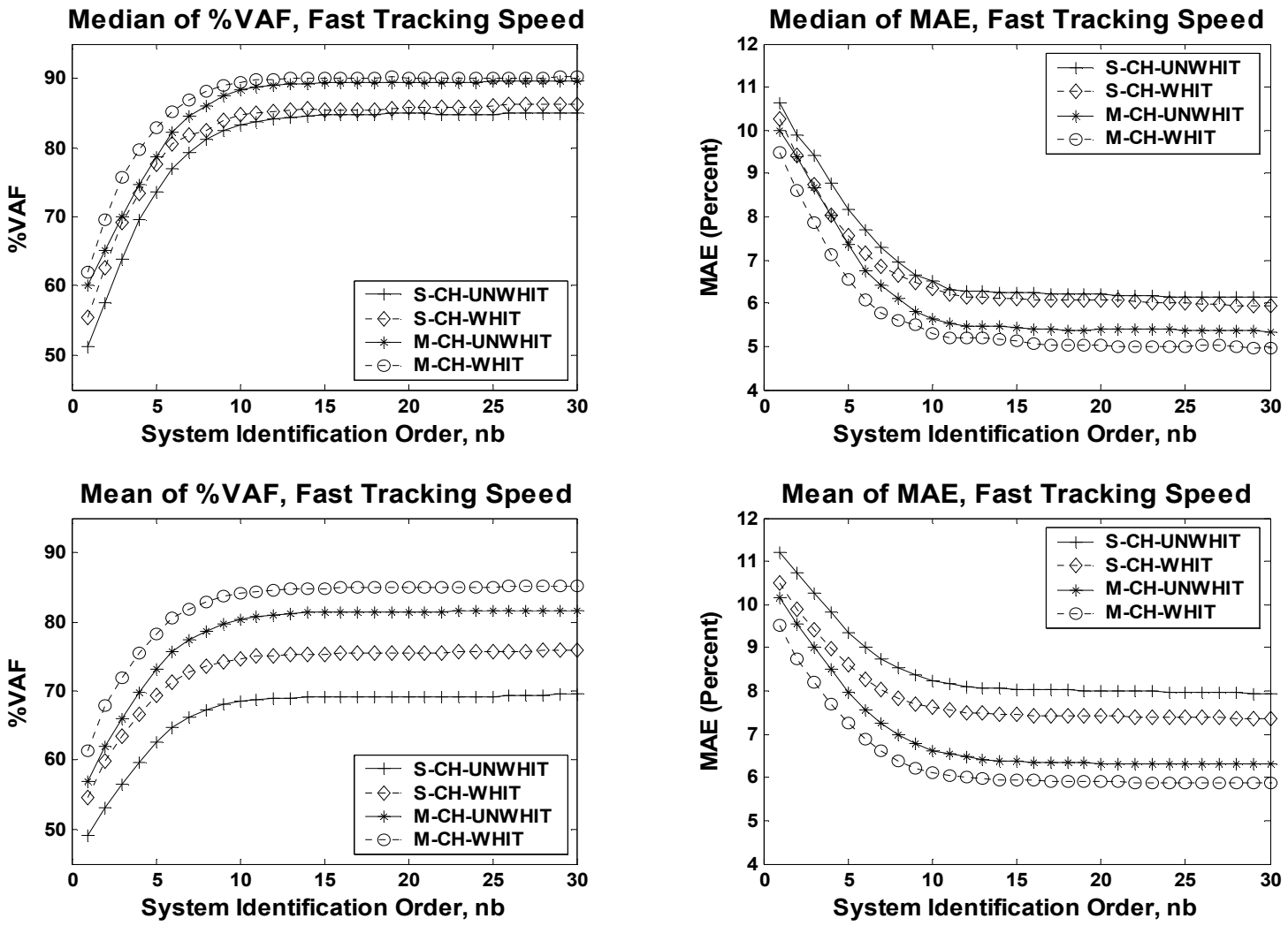

Figure 5.5: Median (left) and Mean (right) of % VAF and % MAE for fast tracking

Assuming that better EMG-torque performance is indicated by higher %VAF and lower % MAE, for all EMG-torque processors the plots show a progressive increase in performance as model order is increased up to about 10–15th order. The improvement seems to stop passing the 20th order and it is expected to eventually decay as the model order starts fitting into the noise. The distribution characteristics (mean, median, and standard deviation) for these data are shown in the following tables.

Table 5.1: Distribution Info of % VAF Values for Each Processor (Fast Tracking)

Processor 1-4	% VAF	n = 1	n = 2	n = 3	n = 4	n = 5	n = 10	n = 15	n = 20
S-CH-UNWHIT	MEDIAN	51.32	57.56	63.86	69.55	73.64	83.29	84.70	84.94
	MEAN	49.17	53.03	56.48	59.65	62.60	68.50	69.07	69.07
	STDEV	43.03	44.17	45.71	47.40	49.31	54.54	56.99	57.41
M-CH-UNWHIT	MEDIAN	55.49	62.65	69.05	73.41	77.57	84.80	85.51	85.79
	MEAN	54.58	59.89	63.47	66.66	69.33	74.73	75.37	75.52
	STDEV	33.73	32.40	32.19	32.13	32.19	32.66	33.03	32.95
S-CH-WHIT	MEDIAN	59.98	65.23	69.99	74.64	78.70	88.31	89.33	89.35
	MEAN	56.91	61.98	66.06	69.81	73.15	80.35	81.39	81.47
	STDEV	31.42	29.99	29.36	28.93	28.75	28.62	29.16	29.49
M-CH-WHIT	MEDIAN	61.99	69.61	75.72	79.60	82.88	89.45	89.98	90.14
	MEAN	61.31	67.92	71.97	75.50	78.33	84.09	84.83	84.97
	STDEV	26.27	22.71	21.21	20.02	19.18	17.84	17.86	17.92

Table 5.2: Distribution Info of % MAE Values for Each Processor (Fast Tracking)

Processor 1-4	% MAE	n = 1	n = 2	n = 3	n = 4	n = 5	n = 10	n = 15	n = 20
S-CH-UNWHIT	MEDIAN	10.64	9.90	9.42	8.77	8.16	6.50	6.24	6.20
	MEAN	11.21	10.73	10.27	9.82	9.36	8.25	8.04	8.01
	STDEV	3.97	3.99	4.09	4.20	4.35	3.97	5.03	5.10
M-CH-UNWHIT	MEDIAN	10.25	9.41	8.74	8.03	7.56	6.34	6.10	6.08
	MEAN	10.51	9.89	10.51	8.99	8.59	7.61	7.45	7.42
	STDEV	3.66	3.59	3.63	3.68	3.75	4.01	4.08	4.10
S-CH-WHIT	MEDIAN	9.98	9.40	8.68	8.02	7.36	5.65	5.43	5.40
	MEAN	10.15	9.55	9.01	8.49	7.98	6.63	6.37	6.33
	STDEV	3.27	3.13	3.09	3.27	3.27	3.35	3.47	3.52
M-CH-WHIT	MEDIAN	9.49	8.62	7.88	7.11	6.56	5.31	5.12	5.02
	MEAN	9.53	8.74	8.20	7.69	7.25	6.12	5.94	5.90
	STDEV	3.01	2.71	2.63	2.59	2.58	2.71	2.76	2.77

As seen, the performance of the processors follows a ranking order with the whitened multiple-channel processor providing the best performance, followed by multiple-channel unwhitened, then single-channel whitened, then single-channel unwhitened. It is also noticed that the median results are higher than the mean, suggesting that there are still a few influential large errors that drag the mean downward.

Finally the PSD of the error is graphed to gain an insight on the origin of the error. The plots show that 80-90% of the error power was within the first 0.5 Hz (shown in the figure below).

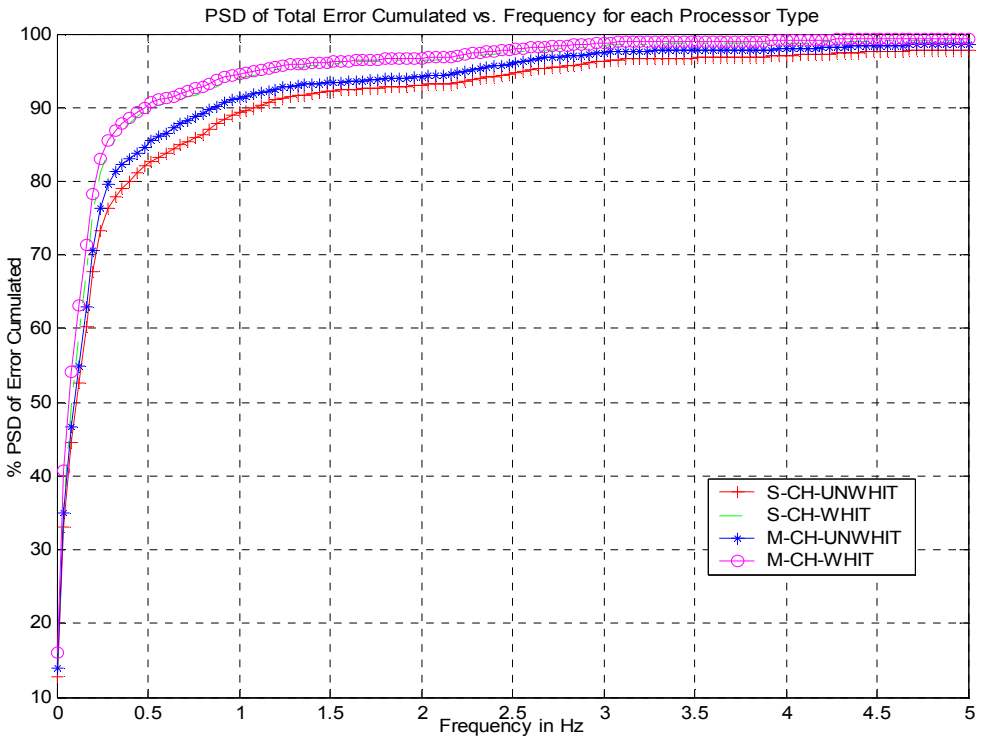

Figure 5.6: PSD of Error Accumulation Rate

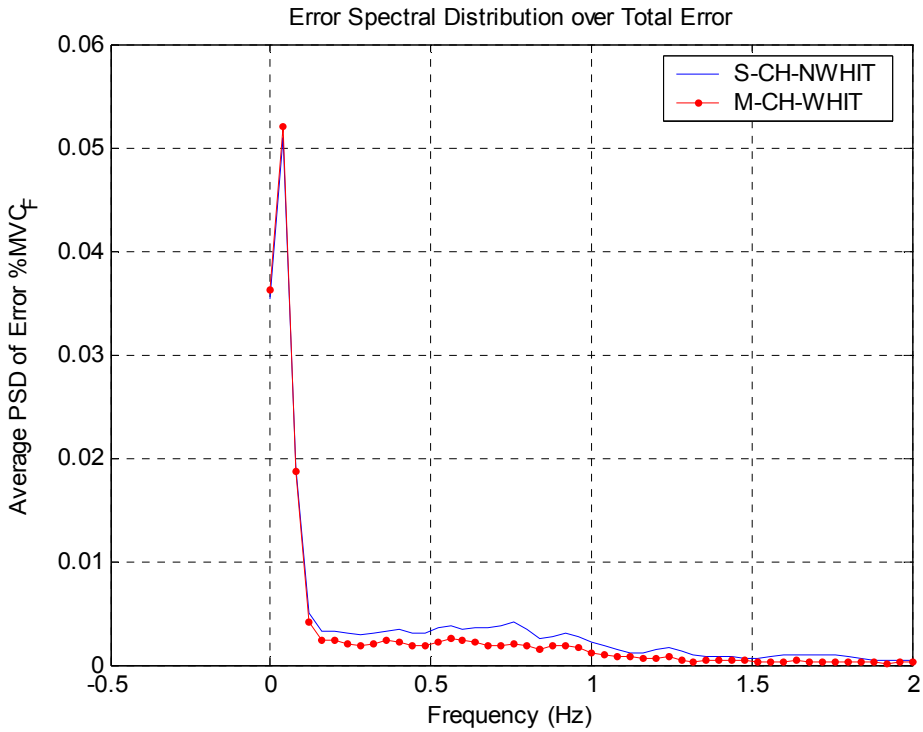

Figure 5.7: The Average PSD of Error as Estimated from Welsh Periodogram

Even though Figure 5.6 suggests that almost all error is accumulated at low frequencies, the windowing effect and the spectral leakage in the Welsh periodogram do not allow further resolution (Figure 5.7). Therefore, it is hard to determine the origin of the remaining error.

After a closer study of the trials with the largest error, it was identified that the error was due to DC shift on the estimated torque as compared to measured one. Moreover, some trials matched were almost perfectly, except for the existence of a positive/negative offset (Figure 5.8).

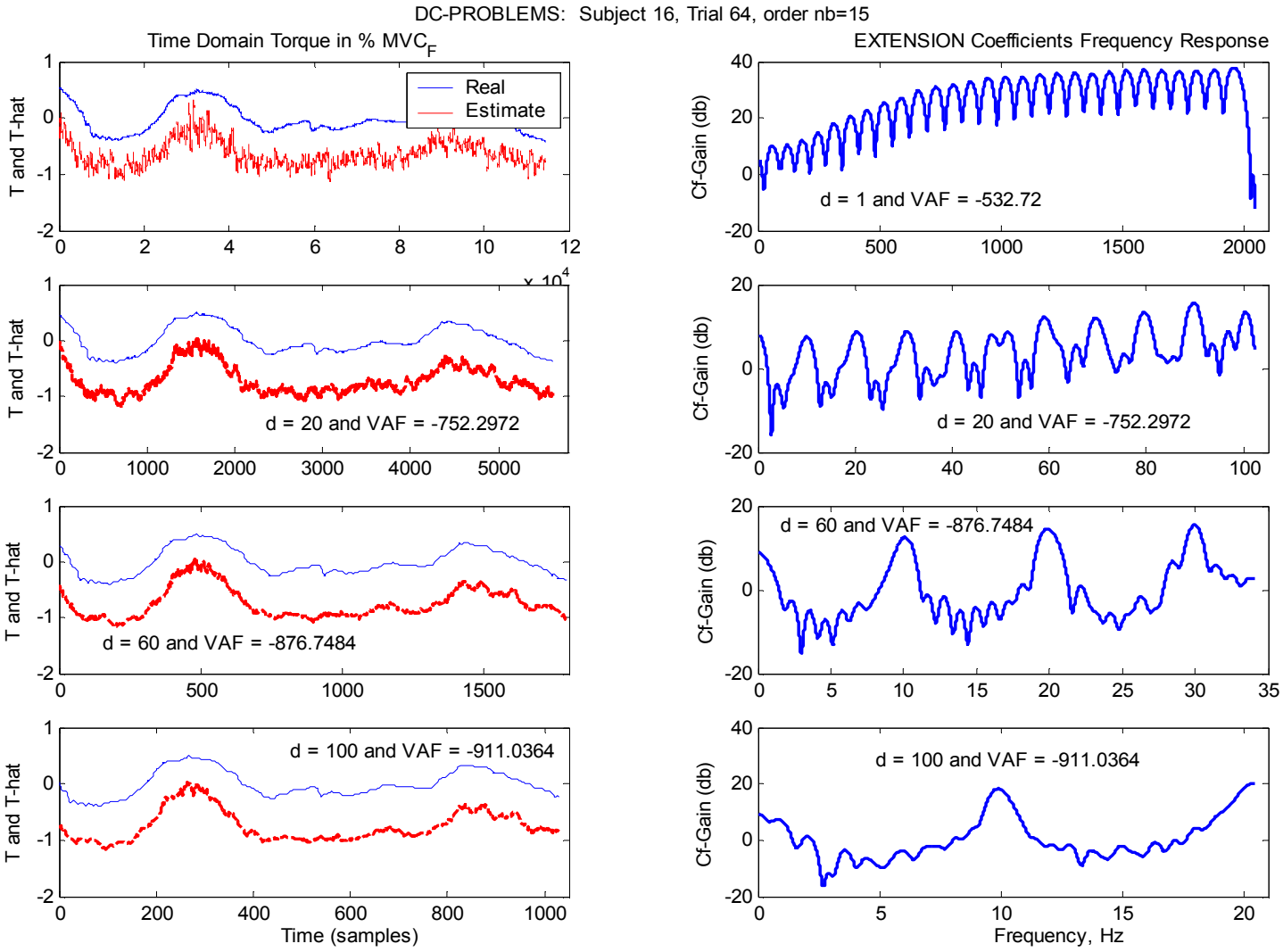

Figure 5.8: High DC Offset Error on Estimated Torque

The figure shows the changes of the estimated torque as the decimation rate is increased (1, 20, 60, 100). The performance of the system indicated by % VAF is getting negatively larger and the DC shift remains as the only apparent error as the AC portion of the estimated torque starts looking exactly like the measured one. Because most of the error power is contained at such low frequencies and the observation of DC shift suggested the same, it can be hypothesized that there is a large amount of error remaining at approximately DC. More investigation of the error plots is required to ensure the hypothesis is correct.

In conclusion, the optimum EMG-torque model (15^{th} order) produced an average error of 6% MVC_F with a %VAF of 90% when the EMG amplitude estimates were obtained from a multiple channel whitened processor. The typical model performance was shown previously in Figure 5.4. The results for the slow tracking speed data were similar and are shown in the appendices. The next largest error in torque estimation seems to be due to a DC offset.

CHAPTER 6. DISCUSSION AND CONCLUSIONS [iii]

This last chapter contains two main sections, the discussion and conclusions. The first part contains the interpretation of the previously anticipated results and then in the second part conclusions are derived from them. In addition, this chapter includes the study limitations and the suggestions for future work.

6.1. DISCUSSION OF RESULTS

The objective of this research was to demonstrate that incorporation of the recent advances in EMG amplitude processors into EMG-torque estimation model produce lower torque prediction errors. The results presented are achieved considering several assumptions on physiological characteristics of the EMG-torque system.

6.1.1. Advances to EMG-torque Estimation

Keeping in mind the main objective, various analyses were conducted to demonstrate that improvement in EMG amplitude processing reduces the estimation error in the torque prediction models. The results derived were consistent with the expectations showing that both whitening and multiple-channel combination of the EMG lead to reduced EMG-torque prediction errors. Even lower errors are obtained when the two techniques are used in combination. Another important result was identifying and resolving the problem of oversampling. This problem arises when EMG data (typical bandwidth from 20–500 Hz) and torque data (typical bandwidth ≈ 5-10 Hz) are simultaneously sampled at the highest required rate. Thus, to preserve information in the

[iii] Parts of this chapter are taken from the paper submitted to the Journal of Biomechanics (attached to Appendices) authored by Clancy, E.A; Bida, O.; Rancourt, D.

EMG data, the torque data are oversampled. If the so overasmpled torque data are used to calibrate EMG-torque models, the resultant transfer functions produce unrealistic gains at frequencies above the typical band of torque data. This issue was observed and solved by decimating the data to a rate of 40.96 Hz that correspond to approximately ten times the highest torque frequency, as recommended by Ljung (1999).

6.1.2. Study Limitations and Future Suggestions

Several assumptions were necessary to complete this project. First, the experimental design consisted of constant-posture non-fatiguing contractions about the elbow. Most practical contractions are more fully dynamic (posture varying). Second, the mechanical model for the elbow treated the joint as a simple hinge, with only one agonist and one antagonist muscle group. This assumption enables the possibility of obtaining one single EMG amplitude estimate using electrodes that are placed anywhere on the skin overlying that muscle group. Consequently, the combination of multiple channels improves the EMG amplitude estimation. In addition, there are only two inputs to the model (EMGamp flexion and EMGamp extension) as opposed to several EMG amplitudes, representative of each individual muscle recording. Increasing the number of muscles in the model would not necessarily improve the EMG amplitude estimates and would increase the complexity of system identification. Another important assumption to consider is that each muscle group contributed only to a certain torque component, such as extensor (flexor likewise) torque was a result of extension (flexion likewise) only. Otherwise, the cross-terms of EMG amplitude had to be incorporated in the model requiring corresponding torque components for mechanical validation.

The EMG-torque model was identified using a zeros-only system design, corresponding to a standard parametric model in the literature (FIR type of ARX model). The reason for selecting a standard linear model was the level of simplicity in the solution and the information available on the system identification techniques. Nonlinear models can be more accurate, for example including hysteresis to capture any systematic differences in the EMG-torque relation between concentric and eccentric contractions. Another advantage is that nonlinear models can potentially capture additional subtle behavior in an EMG-torque relationship such as the electromechanical delay between action potential activation and muscle fiber contraction. Electromechanical delay (EMD) is defined as the temporal delay (26-131 ms) that exists between the onset of muscular activity and the generation of force [Strojnik and Komi, 1998]. In the case of abrupt changes in muscle activation from 0%MVC to 50% MVC, the EMD is a dynamic parameter, hence it is dependent on the number of motor units activated and the fatiguing effects. However, during slow varying force tasks (25% MVC to 50% MVC) the electromechanical delay is constant (60 ms); therefore, its inclusion in the model can be potentially neglected [Vint, McLean, and Harron, 2001].

Although the EMG-torque model for this study included both "AC and DC characteristics" of the system, it is highly recommended in the literature to separate them as part of the data preprocessing routine [Ljung 1999, pp. 458-460]. The investigation of the trials displaying large errors demonstrated that the operating point (DC bias) contaminated in the inputs (EMGamp) and output (torque) data influenced the dynamics of the system, resulting in a DC shift in the estimated torque. Even though many system identification paradigms remove the DC component of each signal prior to identification

so that only the system dynamics (AC portion) are identified, a complete output response (torque) is found by adding the estimated AC portion to a separate estimate of the output DC value. Further studies are suggested, since a complete system response requires separate torque data for model validation and should not have influenced the relative comparison of EMG amplitude processors

The selection of contraction bandwidth that sufficiently excites the system is one of the main issues that need to be addressed in the future. Although tracking targets were at low frequency, 1 Hz is about as fast as subjects were able to track. Faster speeds would require ballistic force trajectories. Therefore, the contraction bandwidth was limited to a 1 Hz tracking target. If higher frequencies are required in the future, the tracking target will need to produce a deterministic trajectory so that ballistic movements (which are inherently faster) can be utilized.

Finally, precautions were taken when recording the data in order to avoid hardware problems such as electrode failures, the distances between the electrodes, and their placement on the skin. The skin was properly prepared to reduce the impedance prior to placing the electrodes; active electrodes rejected the cable motion artefact; digital high pass filters were utilized to eliminate noise due to physiological motion artefact; and the low-pass filters along with decimation attenuated other interferences such as UV lights and power harmonics.

6.2. SUMMARY AND CONCLUSIONS

This research focused on demonstrating that advances in EMG amplitude processors result in EMG-torque model performance improvements. Advances in EMG amplitude estimation were applied to the EMG-torque problem for constant-posture, non-fatiguing,

force-varying contractions about the elbow. Results from 15 subjects showed that EMG whitening and multiple-channel combination both reduce EMG-torque errors and their combination provides an additive benefit. The dynamic relationship between EMG amplitude and joint torque was formulated as a standard linear least squares problem. Using 15^{th}-order and higher linear FIR models, EMG-torque errors with a four-channel, whitened processor produced an average error of 6% MVC_F (%VAF of 90%) at the fast tracking speed. By comparison, the single-channel, unwhitened (conventional) processor produced an average error of 8% MVC_F (%VAF of 68%).

Accomplishing the objective, the issue of non-convergent trials was isolated and resolved by decimating and low pass filtering the data prior to system identification. The EMG amplitude sampling rate was reduced to 40.96 Hz and both EMG amplitude and torque were low-pass filtered at the Nyquist rate, using an 8^{th} order, zero-phase, Butterworth filter. The power spectral density analysis showed that the chosen cutoff frequency of the filter preserved 99.9% of the system power.

Concluding, the primary interest was the influence of different EMG amplitude processors on EMG-torque prediction performance. As such, the study was limited in several manners in order to be able isolate the effect of EMG amplitude without the complexity of less restrictive EMG-torque models. The expectation is that the benefits shown here of improved EMG amplitude processors would transfer to many other EMG-torque modeling problems. Certainly, it now seems justified to progressively release these restrictions and validate these benefits in more general applications in future work.

REFERENCES

[**Armstrong et al., 1982**] T. J. Armstrong, J. A. Foulke, B. S. Joseph, S. A. Goldstein, "Investigation of cumulative trauma disorders in a poultry processing plant." *Amer. Industrial Hyg. Assoc. J.*, vol. 43, no. 2, pp. 103-116, 1982.

[**Agarwal and Gottlieb, 1977**] G.C. Agarwal, G.L. Gottlieb,"Compliance of the human ankle joint." *J Biomech Eng,* vol. 99, pp.166–170, 1977.

[**Basmajian and DeLuca, 1985**] J.V. Basmajian and C.J. De Luca, Muscles Alive: Their Functions Revealed by Electromyography, Williams & Wilkins Company, 1985.

[**Bigland and Lippold, 1954**] B. Bigland, O.C.J Lippold, "The relation between force, velocity and integrated electrical activity in human muscles." *J. Physiol. (Lond)*, vol. 123, pp. 214-224, 1954.

[**Bendat and Piersol, 1986**] J.S. Bendat, A.G. Piersol, Random Data: Analysis and Measurement Procedures, John Wiley, N.Y, 1986.

[**Bobet and Norman, 1990**] "Least-Squares Identification of the dynamic relation electromyogram and joint moment." *J. Biomech.,* vol. 23, no. 12, pp. 1275-6, 1990.

[**Bouchard, 2001**] S. Bouchard, "Relation dynamique entre les signaux electromyogrphiques et le couple au coude lors de contarctions a angles constants." M.S. thesis, Dept. Mech. Eng., Laval Univ., Quebec, Canada 2001.

[**Buchanan et al., 1993**] T. S. Buchanan, M. J. Moniz, J. P. A. Dewald, W. Z. Rymer, "Estimation of muscle forces about the wrist joint during isometric tasks using an EMG coefficient method." *J. Biomech.,* vol. 26, no. 4-5, pp. 547-560, May 1993.

[**Clancy, 1991**] E.A. Clancy, "Stochastic modeling of the relationship between the surface electromyogram and muscle torque." PhD thesis, Dept. Elect. Eng. Comp. Sci., MIT, Cambridge, MA 1991.

[**Clancy, 1999**] E.A. Clancy, "Electromyogram amplitude estimation with adaptive smoothing window length." *IEEE Trans. Biomed. Eng.,* vol. 46, no. 6, 1999.

[**Clancy, 2004**] E.A. Clancy. EMG amplitude estimation toolbox: User's guide. Alpha version 0.04. Available on-line at: http://ece.wpi.edu/~ted/emg_tool.htm. Accessed January 30, 2005.

[**Clancy et al., 2001**] E.A. Clancy, S. Bouchard, D. Rancourt, "Estimation and application of EMG amplitude during dynamic dontractions." *IEEE Eng. Med. Bio. Mag.*, vol. 20, no.6, Nov. - Dec. 2001.

[**Clancy et al., 2004**] E.A. Clancy, D. Farina, G. Filligoi, "Single Channel Techniques for Information Extraction from the Surface EMG," in *Electromyography: Physiology, Engineering, and Noninvasive Applications,* Roberto Merletti and Philip A. Parker, eds., John Wiley & Sons, Inc., Hoboken, New Jersey, pp. 133–168, 2004.

[**Clancy and Farry, 2000**] E.A. Clancy and K.A. Farry, "Adaptive whitening of the electromyogram to improve amplitude estimation." *IEEE Trans. Biomed. Eng.*, vol. 47, no. 6, June 2000.

[**Clancy and Hogan, 1995**] E.A Clancy, N. Hogan, "Multiple site electromyograph amplitude estimation." *IEEE Trans. Biomed. Eng.*, vol. 42, pp. 203–211, 1995.

[**Clancy and Hogan, 1997**] E.A. Clancy and N.Hogan, "Relating agonist-antagonist electromyograms to joint torque during isometric, quasi-isotonic, nonfatiguing contractions." *IEEE Trans. Biomed. Eng.*, vol. 44, no. 8, June 2000.

[**Clancy, Morin, and Merletti 2002**] E.A. Clancy, E.L. Morin, R. Merletti, "Sampling, noise-reduction and amplitude estimation issues in surface electromyography." *J. Electromyog. Kines.,* vol. 12, pp 1–16, December 2002.

[**DeLuca, 2002**] C.J. De Luca, "Surface electromyography: detection and recording" DelSys Inc. Copyrighted 2002

[**Dowling, 1997**] J.J Dowling, "The use of electromyography for the noninvasive prediction of muscle forces." *Sports Med.*, vol. 24, no. 2, pp. 82-96, Aug. 1997.

[**Farina, Merletti, and Enoka, 2004**] D. Farina, R. Merletti, R.M. Enoka, "The extraction of neural strategies from the surface EMG." *J. Appl. Physiol.* vol. 96 pp. 1486-1495, 2004.

[**Grant et al., 1994**] K. A. Grant, D. J. Habes, V. Putz-Anderson, "Psychophysical and EMG correlates of force exertion in manual work." *Int. J. Industrial Ergonomics,* vol. 13, pp. 31-39, 1994.

[**Gottlieb and Agarwal, 1971**] G.L. Gottlieb and G.C. Agarwal, "Dynamic relationship between isometric muscle tension and the electromyogram in man." *J. Appl. Physiol.*, vol. 30, pp. 345 – 351, 1971.

[**Gottlieb et al., 1997**] G.L. Gottlieb, Q. Song, G.L. Almeida, D. Hong, D. Corcos, "Directional control of planar human arm movement." *J. Neurophys.,* vol. 78, pp. 2985-2998, 1997

[**Hannerz, 1974**] J. Hannerz, "Discharge properties of motor units in relation to recruitment order in voluntary contraction." *Acta Physiol. Scand*., vol. 91, pp. 374–384, 1974.

[**Hasan and Enoka, 1985**] Z. Hasan, R. M. Enoka, "Isometric torque angle relationship and movement related activity of human elbow flexors: Implications for the equilibrium-point hypothesis." *Exp. Brain Res.,* vol. 59, pp. 441-450, 1985.

[**Hof and Van Den Berg, 1981**] A.L. Hof, Jw. Van den Berg, "EMG to force processing I: An electrical analogue of the Hill muscle model." *J. Biomechanics* vol. 14, no. 11, pp. 747–758, 1981.

[**Hogan and Mann, 1980a**] N. Hogan and R.W. Mann, "Myoelectric signal processing: optimal estimation applied to electromyography-Part I: Derivation of the optimal myoprocessor." *IEEE Trans. Biomed Eng.*, vol. BME-27, pp. 382-395. July 1980.

[**Hogan and Mann, 1980b**] N. Hogan and R.W. Mann, "Myoelectric signal processing: optimal estimation applied to electromyography-Part I: Derivation of the optimal myoprocessor." *IEEE Trans. Biomed Eng.*, vol. BME-27, pp. 396-410. July 1980.

[**Hughes and Chaffin, 1997**] R. E. Hughes, D. B. Chaffin, "Using principal-components regression to stabilize EMG-muscle force parameter estimates of torso muscles." *IEEE Trans. on Biomed. Eng.,* vol. 44, no. 7, pp. 639-642, 1997.

[**Inman et al., 1952**] V.T. Inman, H.J. Ralston, J.B.C.M Saunders, B. Feinstein, E.W. Wright, "Relation of human electromyogram to muscular tension." *Electroencephol. and Clin. Neurophys.* vol. 4, 187–194, 1952.

[**Kirsch, Kearney, and Crago, 1994**] R.F. Kirsch, R.E. Kearney, P.E. Crago, "Dynamic stiffness measurements and control movement." *IEEE 16th Ann. Int. Conf. Proc.,* vol.1, pp. 428-429, November 1994.

[Kolman and Hill, 2001] B. Kolman, D. R. Hill, "*Introductory Linear Algebra with Applications*", 7th ed. Prentice Hall, New Jersey, pp.327-339, 2001.

[**Laursen et al., 1998**] B. Laursen, B. R. Jensen, G. Nemeth, G. Sjogaard, "A model predicting individual shoulder muscle forces based on relationship between electromyographic and 3D external forces in static position." *J. Biomech.,* vol. 31, pp. 731-739, 1998.

[**Lawrence and DeLuca, 1983**] J.H.Lawrence, C.J De Luca, "Myoelectric signal versus force relationship in different human muscles." *J. Appl. Physiol.,* vol. 54, pp. 1653-1659, 1983.

[**Lamb and Hobart, 1992**] R. Lamb, D. Hobart, "Selected topics in surface electromyography for use in the occupational settings: exepert perspectives", (CH 2), *U.S. Department of Health and Human Service (CDC) – NIOSH*, March 2002.

[**Lindstrom and Magnusson, 1977**] J. Lindstrom, R. T. Magnusson, "Interpretation of myoelectric power spectra: A model and its application." *Proceedings of the IEEE*, vol. 65, pp 653-662, 1977.

[**Ljung, 1999**] L. Ljung, System Identification: Theory for the User, Upper Saddle River, NJ: Prentice-Hall, 1999.

[**Milner-Brown and Stein, 1975**] H. S. Milner-Brown, R. B. Stein, "The relation between the surface electromyogram and muscular force." *J. Physiol.*, vol. 246, pp. 549-569, 1975.

[**McGill, 1992**] S.M. McGill, "A myoelectrically based dynamic three-dimensional model to predict loads on lumbar spine tissues during lateral bending." *J. Biomech.*, vol. 25, no. 4, pp. 395-414, Apr.1992.

[**Merletti, 1999**] R. Merletti, "Standards for Reporting EMG Data." *J. Electromyography Kinesiology,* 1999.

[**Moritani and DeVries, 1978**] T. Moritani, H. DeVries, "Reexamination of the relationship between the surface integrated electromyogram (IEMG) and force of isometric contraction." Amer. J. Phys. Med., vol. 57, no. 6, pp. 263-277, 1978.

[**Nussbaum, Chaffin, and Martin, 1995]** M. A. Nussbaum, D. B. Chaffin, B. J. Martin, "A back-propagation neural network model of lumbar muscle recruitment during moderate static exertions." *J. Biomech*., vol. 28, no. 9, pp. 1015-1024, 1995.

[**Papoulis, 2002**] A. Papoulis, Probability, Random Variables, and Stochastic Processes, 4th edition, McGraw Hill, 2002.

[**Perry and Bekey, 1981**] J. Perry, G. A Bekey, "EMG-force relationships in skeletal muscle." *CRC Critical Rev. in Biomed.* Eng., pp. 1-22, December 1981.

[**Ray and Guha, 1983**] G.C. Ray, S.K. Guha, "Relationship between the surface e.m.g. and muscular force." *Med. Biol. Eng. Comput.*, vol. 21, no. 5, pp. 579-586, Sept. 1983

[**Solmonow et al., 1986**] M. Solomonow, A. Guzzi, R. Baratta, H. Shoji, R. D'Ambrosia, "EMG-force model of the elbow's antagonistic muscle pair: The effect of joint position, gravity and recruitment." *Am. J. Physic. Med.,* vol. 65, pp. 223–244, 1986.

[**Solmonow et al., 1990**] M. Solomonow, R. Baratta, H. Shoji, R. D'Ambrosia, "The EMG-force relationships of skeletal muscle; dependence on contraction rate, and motor units control strategy." *Electromyog.r Clin. Neurophysiol.,* vol. 30, no. 3, pp. 141-152, 1990.

[**Sommerich et al., 1998**] C. M. Sommerich, W. S. Marras, M. Parnianpour, "A method for developing biomechanical profiles of hand-intensive tasks." *Clinic. Biomech.*, vol. 13, pp. 261-271, 1998.

[**Stokes, Moffroid, Rush, and Haugh, 1989**] I. A. F. Stokes, M. Moffroid, S. Rush, L. D. Haugh, "EMG to torque relationship in rectus abdominis muscle." Spine, vol. 14, no. 8, pp. 857-61, 1989.

[Strojnik and Komi, 1998] V. Strojnik, P. V. Komi, "Neuromuscular fatigue after maximal stretch-shortening cycle exercises." J. Appl. Physiol., Vol. 84, Issue 1, pp. 344-350, 1998.

[**Thelen et al., 1994**] D.G. Thelen, A.B. Schultz, S.D. Fassois, J.A. Ashton-Miller, "Identification of dynamic myoelectric signal-to-force models during isometric lumbar muscle contractions." *Journal of Biomechanics*, vol. 27, pp. 907–919, 1994.

[**Thelen, 2003**] D.G. Thelen, "Adjustment of muscle mechanics model parameters to simulate dynamic contractions in older adults." *J. Biomech. Eng.,* vol. 125, pp. 70-77, 2003.

[Valero-Cuevas et al., 2003] F.J Valero-Cuevas, M.E. Johanson, J.D. Towles, "Towards a realistic biomechanical model of the thumb: the choice of kinematic description may be more critical than the solution method or the variability/uncertainty of musculoskeletal parameters." *J Biomech*, vol. 36, pp. 1019-1030, 2003.

[Vint, McLean, and Harron, 2001] P.F. Vint, S.P. McLean, G.M. Harron, "Electromechanical delay in isometric actions initiated from non-resting levels." Med. & Sci. in Sports & Exercise, vol. 33, issue 6 pp. 978-983. 2001.

[**Vredenbregt and Rau, 1973**] J. Vredenbregt, G. Rau, "Surface EMG in relation to force, muscle length and endurance." *New Develop. EMG Clin. Neurophys.,* vol. 1, pp. 607-622, 1973.

[**Westwick, 1995**] D.T. Westwick, Methods for the Identification of Multiple-Input Nonlinear Systems. Dept. EE Biomed. Eng., McGill University, Montreal, Quebec, Canada, 1995. http://www.enel.ucalgary.ca/People/Westwick/Publications/

[**Woods and Bigland-Ritchie, 1983**] J.J. Woods, B. Bigland-Ritchie, "Linear and non-linear surface EMG/force relationships in human muscles: An anatomical/functional argument for the existence of both." *Am. J. Phys. Med.*, vol. 62, no. 6, pp. 287-299, 1983.

[**Wyss and Pollak, 1984**] J.P. Wyss, V.A. Pollak "Surface electromyogram/muscle force: a muscle model based on RMG peaks." Eng. Med., vol. 13, no. 1, pp. 27-33, 1984.

[**Zuniga and Simons, 1969**] E.N. Zuniga, D.G. Simons, "Nonlinear relationship between averaged electromyogram potential and muscle tension in normal subjects." *Arch. Phys. Med. and Rehab.*, 613-620, November 1969.

APPENDICES: ADDITIONAL INFORMATION, PLOTS, AND FIGURES

I. LBXXXX EXPERIMENT DATA FILE DESCRIPTION

The file name code is LBSSTT where SS stands identifies the subject (02-05, 07-10, 12, 13, 16, 17, 18, 20, 21) and TT identifies the experiment trial (20-29, 40-49, 60-69). There are 15 subjects and 3 sets of 10 trials per subject. The different trials within a set were obtained using different feedback mechanisms and bandwidths for the tracking signal. One out of four trials was used to train the EMG-torque model the other four to test it.

Table 0.1: Trial ID Name Codes

TRIAL ID (TT)	Feedback Mechanism	Target Bandwidth (Hz)
20 (train)	EMG, Single Channel Unwhitened	0.25
21 (test)	EMG, Multiple Channel Unwhitened	0.25
22 (test)	EMG, Single Channel Whitened	0.25
23 (test)	EMG, Multiple Channel Whitened	0.25
24 (test)	Dynamometer	0.25
25 (train)	EMG, Single Channel Unwhitened	1
26 (test)	EMG, Multiple Channel Unwhitened	1
27 (test)	EMG, Single Channel Whitened	1
28 (test)	EMG, Multiple Channel Whitened	1
29 (test)	Dynamometer	1
40 (train)	EMG, Single Channel Unwhitened	0.25
41 (test)	EMG, Multiple Channel Unwhitened	0.25
42 (test)	EMG, Single Channel Whitened	0.25
43 (test)	EMG, Multiple Channel Whitened	0.25
44 (test)	Dynamometer	0.25
45 (train)	EMG, Single Channel Unwhitened	1
46 (test)	EMG, Multiple Channel Unwhitened	1
47 (test)	EMG, Single Channel Whitened	1
48 (test)	EMG, Multiple Channel Whitened	1
49 (test)	Dynamometer	1
60 (train)	EMG, Single Channel Unwhitened	0.25
61 (test)	EMG, Multiple Channel Unwhitened	0.25
62 (test)	EMG, Single Channel Whitened	0.25

63 (test)	EMG, Multiple Channel Whitened	0.25
64 (test)	Dynamometer	0.25
65 (train)	EMG, Single Channel Unwhitened	1
66 (test)	EMG, Multiple Channel Unwhitened	1
67 (test)	EMG, Single Channel Whitened	1
68 (test)	EMG, Multiple Channel Whitened	1
69 (test)	Dynamometer	1

Each of the files contained 16 channels from the DAQ describing the electrode positions as follows. The table lists only the channel used for this study.

Table 0.2: A/D Channel Name Codes

A/D Channel	Contents
1	EMG: Biceps, most lateral location
2	EMG: Biceps, lateral center
3	EMG: Biceps, medial center
4	EMG: Biceps, most medial location
8	EMG: Triceps, most medial location
9	EMG: Triceps, medial center
10	EMG: Triceps, lateral center
11	EMG: Triceps, most lateral
16	Dynamometer

II. OPTIONAL PROPERTIES FOR AMPLITUDE ESTIMATION ALGORITHM

EMG amplitude estimation as taken from the EMG toolbox User Manual.

Syntax : EMGamp = e_amp(EMGin, EMGinfo)

EMGinfo – obtained from calibration

EMGin – input EMG channel (CH 2 for flexion and CH 9 for extension) or Multiple Channels (CH 1:4 for flexion and CH 8:11 for extension)

Calibration for EMG amplitude estimation as in EMG toolbox User Manual.

Syntax: EMGinfo = e_cal(SandNmat, sCal, NoiseMat, SampFreq [, 'PropertyName', PropertyValue, ...]

SandNmat - Noisy signal Matrix (Input Channel). This signal is specifically recorded for calibration process. Trial 10 is used for flexion and trial 12 for extension. The channels are the same as the input channels shown for EMGin.

NoiseMat – Noise recorded per trial, rest Trial 15 (take corresponsing channel) For example: NoiseMat for flexion is trial 15 (CH 2 for single-channel and CH 1:4 for multiple-channel) and for extension is still trial 15 but different channels.

Properties as set of this project:

sCal: 0.5

SampFreq: 4096 Hz

High Pass Filter Settings

Causality 'Flag': Default value is 'Noncausal'.

HpassFlag 'Flag': Default value is 'Filter'.

HpassOrder Order: Default value is set by e_h_pass() and Order = 5.

HpassWn: Default value is set to correspond to 15 Hertz.

Whitening Filter Settings

WhiteFlag 'Flag': Depends, S-CH-WHIT and M-CH-WHIT is ‘ON’ else ‘OFF’.

WhiteEdges EdgeString: Default is set by e_whiten().

WhiteMaxGain MMaxGain: Default is set by e_cal_wh().

WhiteNfft NNfft: Default is set by e_cal_wh().

WhiteOrder Order: Default is set by e_cal_wh().

White_sSpec sSpec: Default is set by e_cal_wh().

WhiteSum SumString: Default is set by e_whiten().

WhiteSmFilt FiltOption: Not Used.

WhiteSmFilt = 'MAV':

WhiteSmFixWin Window = 1024 = 250ms.

Multiple Channel Combination Setting

UncorrFlag 'Flag': Default is 'GainOnly', if multiple channels.

Demodulation Settings

DemodFlag 'Flag': Default value is 'On'.

DemodM M: Default d = 1 (MAV)

Smoothing Filter Setting

SmoothFilt FiltOption: 'butter'

SmoothEdges EdgeString: Default value is set by e_smooth().

SmoothWn: 0 < Wn < 1= > Wn = 20/2048 which is 20Hz

SmoothOrder: Order = 8

For example EMGinfo for Extension in the case of Single Channel Processor

```
EMGinfoExt = e_cal(SandNmatE, 0.5, NmatE, 4096, 'WhiteFlag', Wflag, 'WhiteSmFilt',
        'MAV', 'WhiteSmFixWin', 1024);
```

The code looks exactly the same for all the other cases. For more information on the settings and the EMG toolbox functionalities refer to the User Manual created and maintained by Clancy (2004) found in the website:

http://ece.wpi.edu/~ted/emg0_04/front.html

III. EXTRA FIGURES AND PLOTS

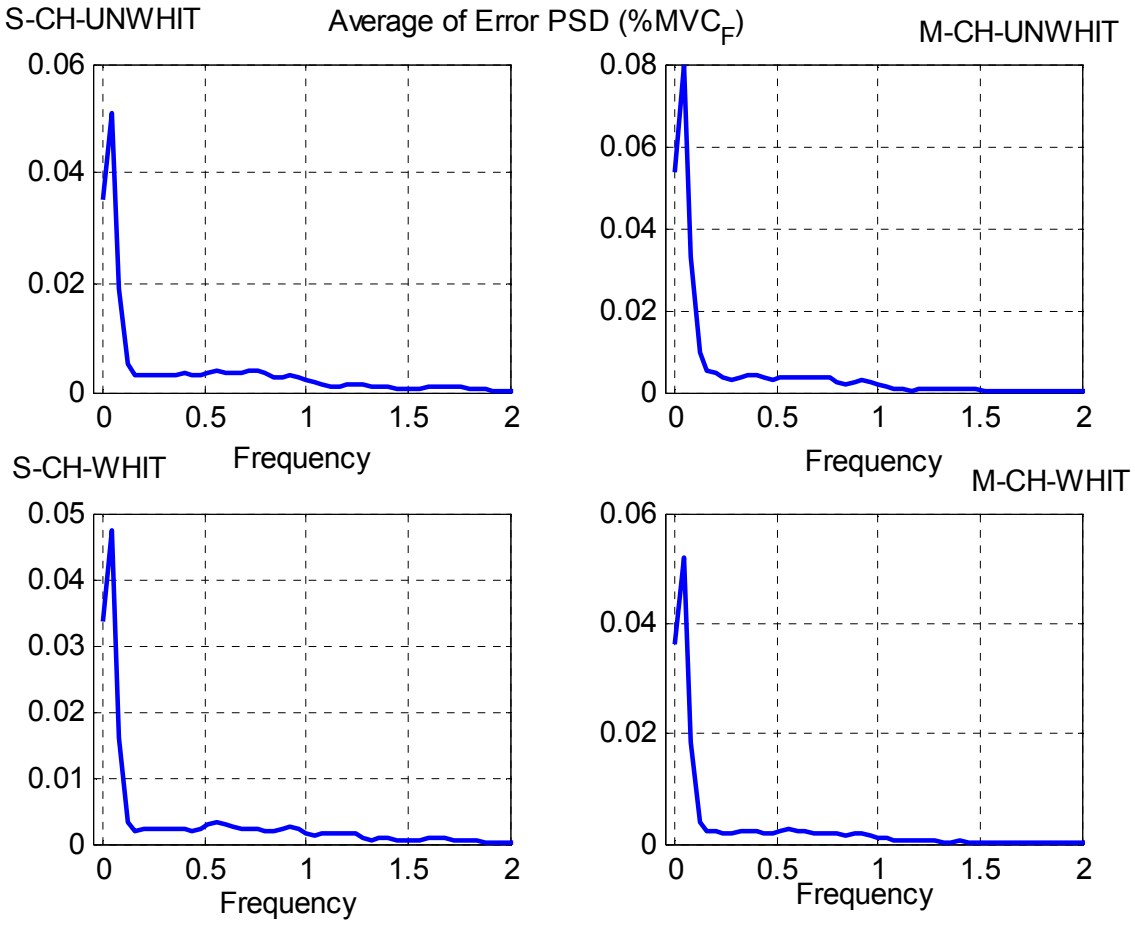

Figure 0.1: Estimation Error PSD (Welsh Periodogram) for all 4 Processors

The power density spectra (PSD) of estimation error are approximated using Welsh periodogram for all four processors. Figure 0.1 is used to support the argument that the estimation error for all processors behaves similarly in frequency domain. Figure 5.7 shows only two of the processors (s-ch-whit, m-ch-whit).

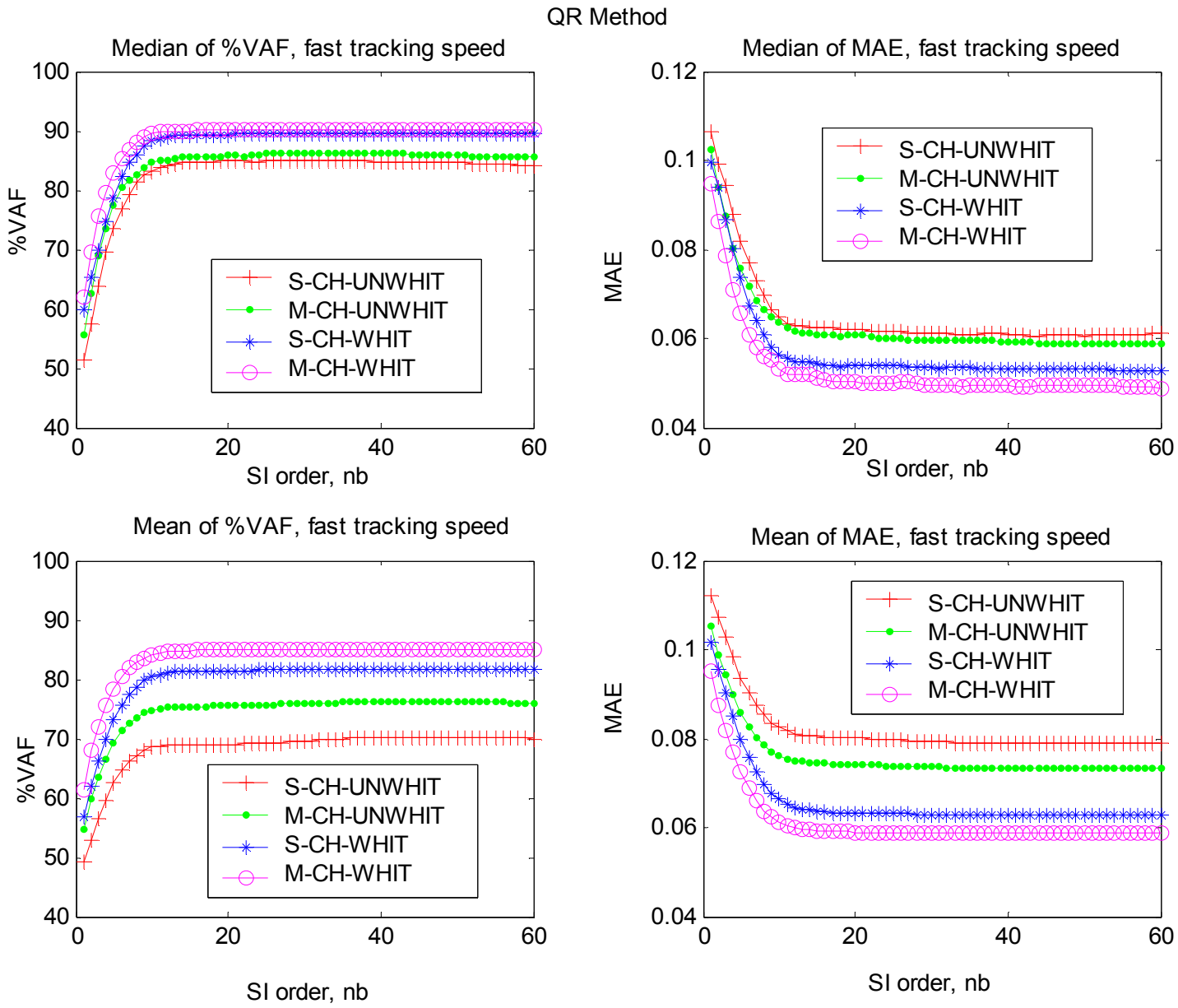

Figure 0.2: System Performance (% VAF & MAE) using QR Factorization (Fast Tracking)

The system performance versus system ID order using QR factorization to compute the inverse of the matrices is given to support the argument that the pseudo-inverse and the QR factorization give equal results. Figure 0.2 is contrasted with Figure 5.5 and the results seem to match perfectly.

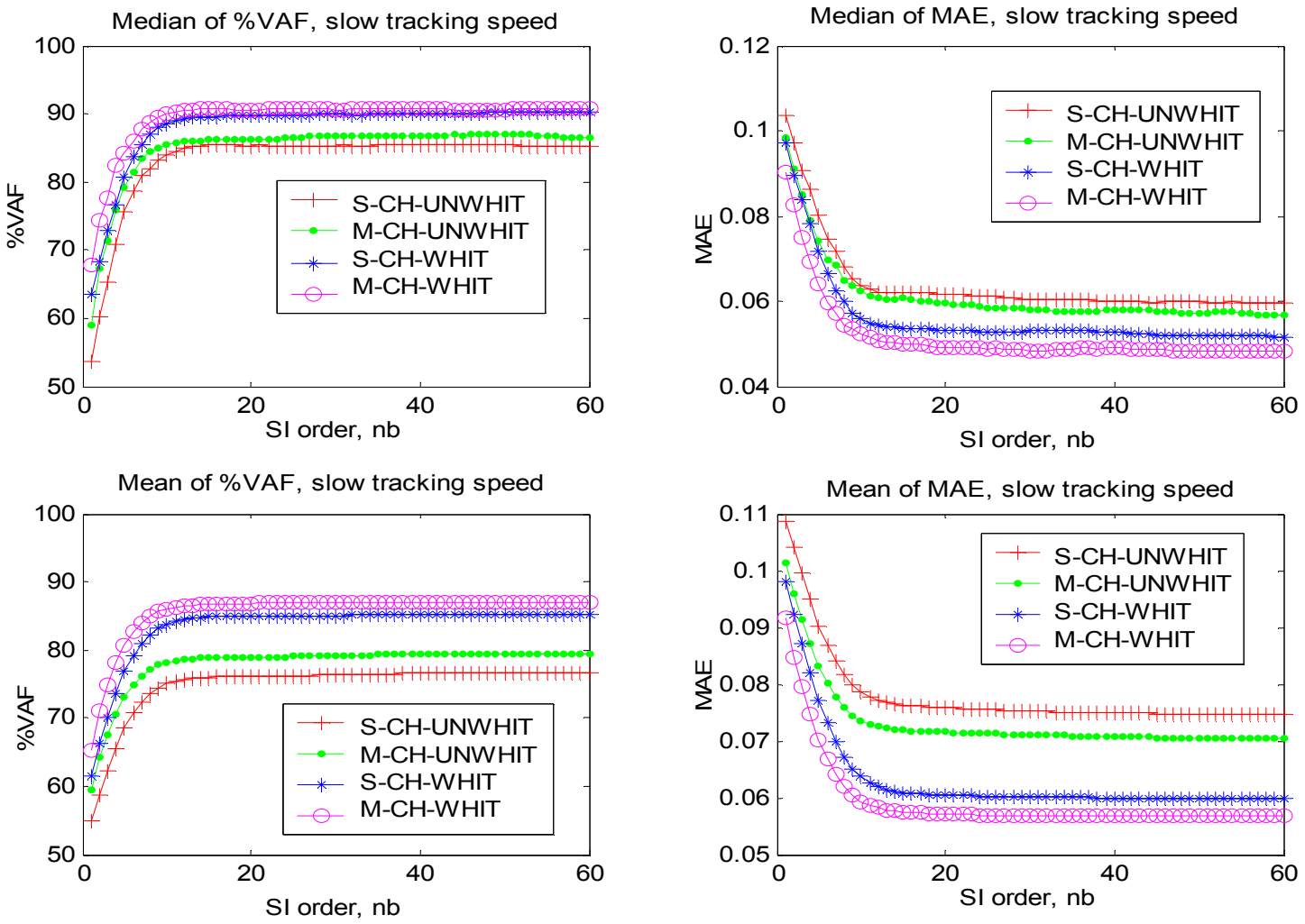

Figure 0.3: System Performance (% VAF & MAE) using Pseudo-Inverse (Slow Tracking)

Figure 0.3 is contrasted with Figure 5.5 and the processor performance ranking order seems to follow the same pattern. The model gives better results for slow target tracking tasks which is consistent with the statement that the subjects have trouble tracking ballistic random trajectories. Regardless, the positive influence of EMG amplitude processor on the EMG-torque model performance is proven for both cases (fast and slow bandwidth signal target).

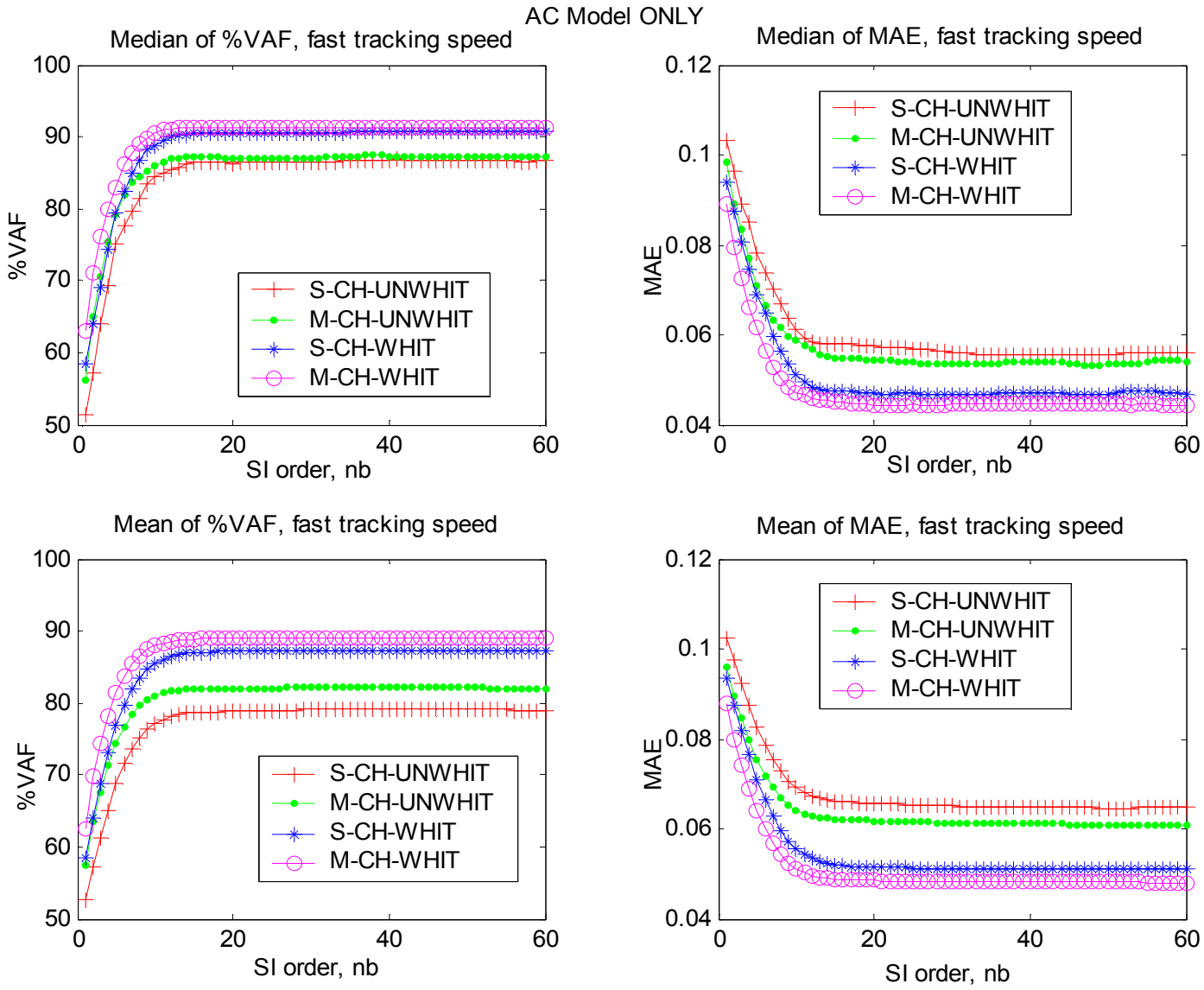

Figure 0.4: System Performance (% VAF & MAE) using AC part of EMG Amplitudes (Fast Tracking + PINV)

Figure 0.4 is contrasted with Figure 0.3 and Figure 5.5. The processor performance ranking order seems to follow yet the same pattern. The model gives even better results when only the AC portion of EMG recordings and measured torque are used in the system. This is another observation toward solving the remaining problems and leading again to the assumption that the inclusion of DC in the models is erroneous.

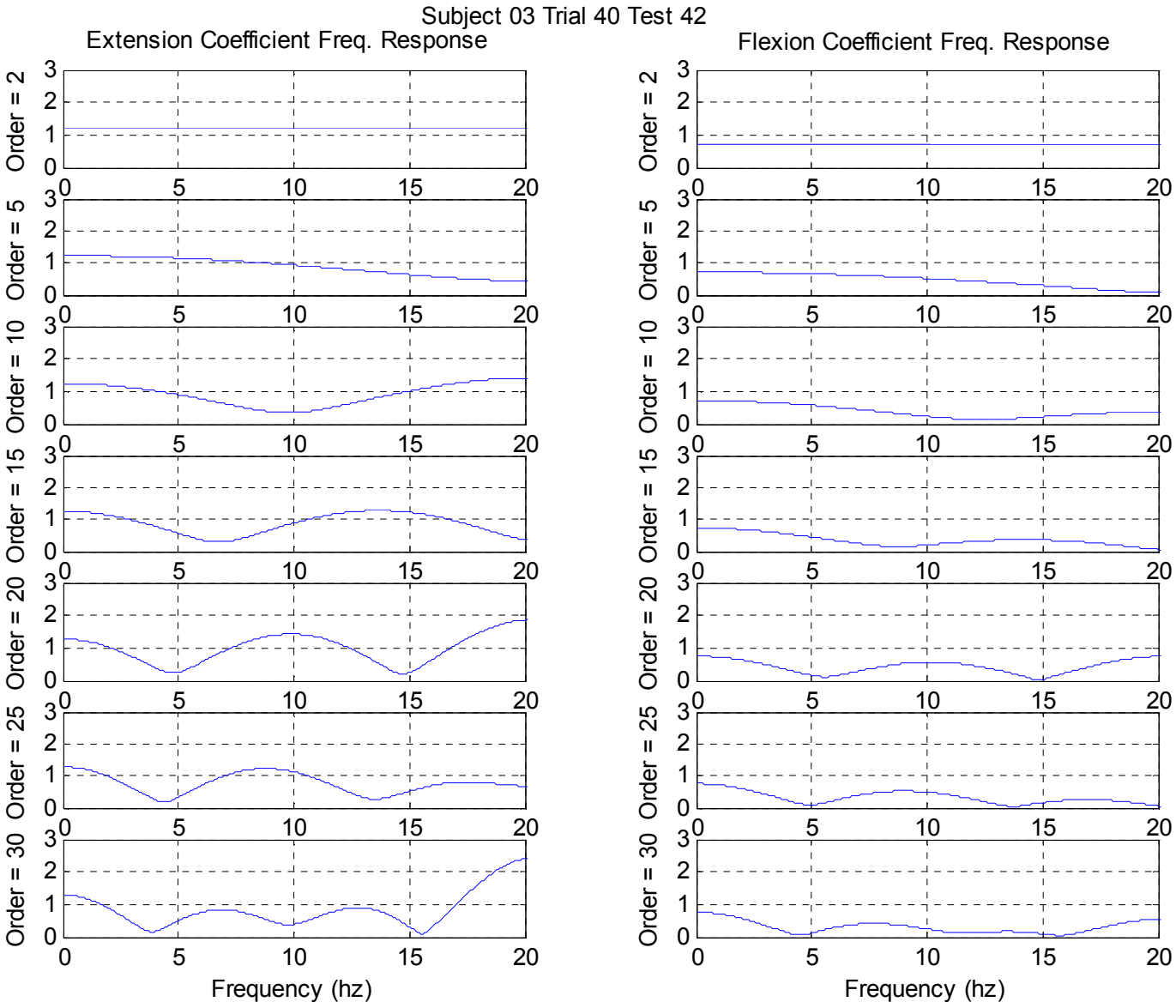

Figure 0.5: Coefficients Frequency Response for a typical EMG-Torque model (Slow Tracking)

The most important factor observed in this figure is the shape change as the number of zeros (model order) is increased. Notice that as the order of the system passes the value ten little or no improvement is seen within 5Hz (bandwidth of the system). Higher orders seem to add shape to frequencies outside the system bandwidth. This observation is consistent with the system saturation after 15^{th} order seen in many of the plots shown above.

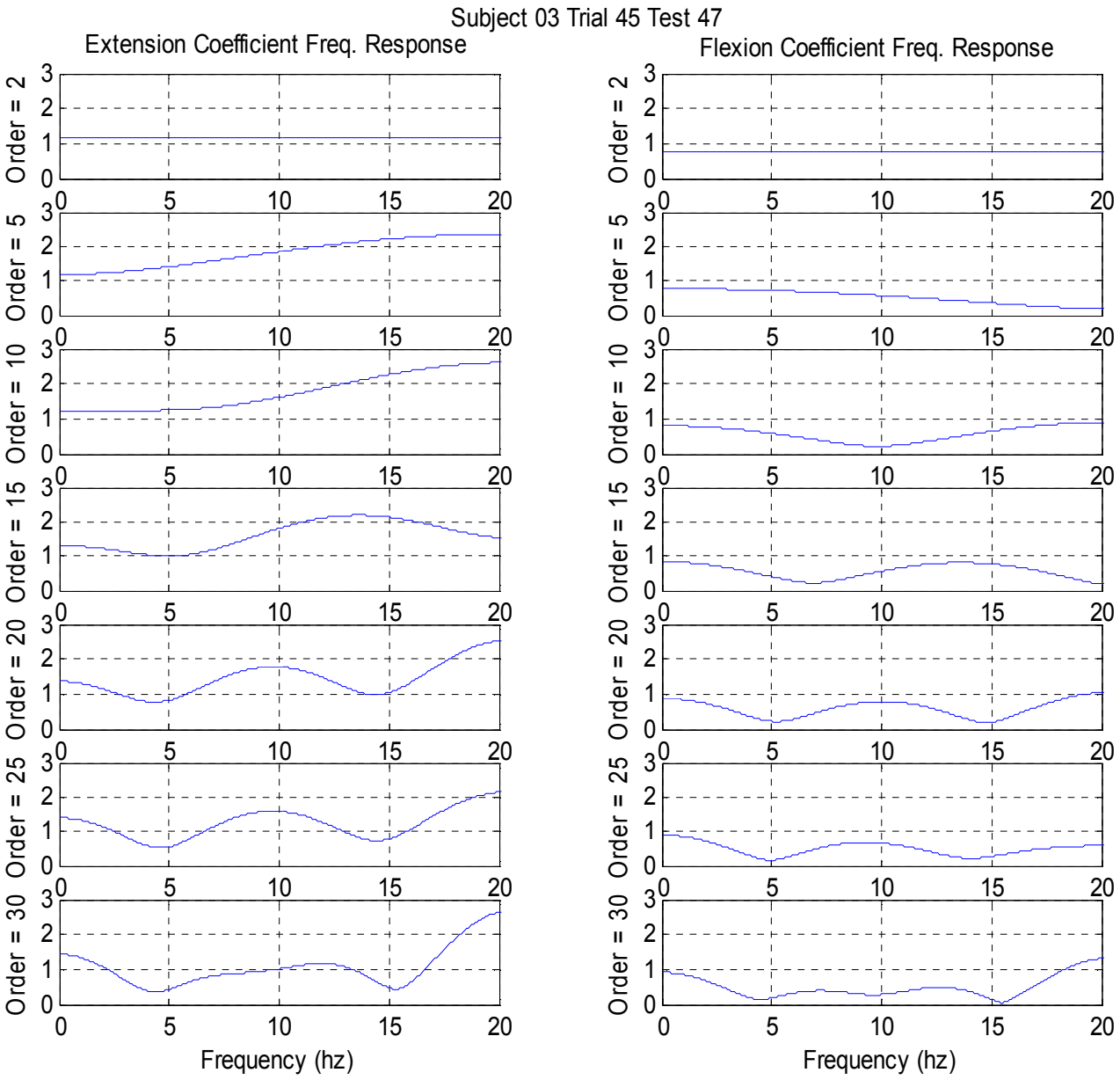

Figure 0.6: Coefficients Frequency Response for a typical EMG-Torque model (Fast Tracking)

This plot is equivalent with Figure 0.5 for fast target tracking tasks. Similarly, as order increases more shape is added to the response. In this plot it is also observed that during low order the fast later zeros do not leave time for the previous ones to create the dip effect. This is observed on the high-pass look alike response for second and fifth orders.

IV. PAPER SUBMITTED TO THE JOURNAL OF BIOMECHANICS

Influence of advanced electromyogram (EMG) amplitude processors on EMG-to-torque estimation during constant-posture, force-varying contractions

by

E.A. Clancy [a,*], O. Bida[b], D. Rancourt[c]

[a] *Department of Electrical and Computer Engineering, Department of Biomedical Engineering, Worcester Polytechnic Institute, 100 Institute Rd., Worcester, MA, 01609, USA*

[b] *Department of Electrical and Computer Engineering, Worcester Polytechnic Institute, Worcester, MA, USA*

[c] *Department of Mechanical Engineering, University of Sherbrooke, Sherbrooke, PQ, Canada*

Edward (Ted) A. Clancy (Corresponding Author)

Department of Electrical and Computer Engineering

Worcester Polytechnic Institute

100 Institute Road, Worcester, MA 01609 USA

Tel. (508) 831-5778, Fax. (508) 831-5491, E-mail: ted@wpi.edu

Abstract

Numerous studies have investigated the relationship between surface EMG and torque exerted about a joint. These studies have used conventional EMG amplitude (EMGamp) processing, such as rectification followed by low pass filtering, to pre-process the EMG before relating it to torque. Recently, advanced EMGamp processors that incorporate signal whitening and multiple-channel combination have been shown to significantly improve EMGamp processing. In this study, we compared the performance of EMGamp-torque estimators with and without these advanced EMGamp processors. Fifteen subjects produced constant-posture, nonfatiguing, force-varying contractions about the elbow while torque and biceps/triceps EMG were recorded. EMGamp was related to torque using a linear FIR model. Both whitening and multiple-channel combination reduced EMG-torque errors and their combination provided an additive benefit. Using a 15^{th}-order linear FIR model, EMG-torque errors with a four-channel, whitened processor averaged 6% of maximum voluntary contraction (or 90% of variance accounted for). By comparison, the equivalent single-channel, unwhitened (conventional) processor produced an average error of 8% of maximum voluntary contraction (variance accounted for of 68%). In addition, the study describes the occurrence of spurious peaks in estimated torque when the torque model is created from data with a sampling rate well above the bandwidth of the torque. This problem occurs when the torque data are sampled at the same rate as the EMG data. The problem is corrected by decimating the EMGamp prior to relating it to joint torque, in our case to an effective sampling rate of 40.96 Hz.

Keywords: EMG, EMG amplitude, Torque, EMG-torque model, Optimal sampling rate